Renewable Energy 208 (2023) 512–537

Contents lists available at ScienceDirect

Renewable Energy

journal homepage: www.elsevier.com/locate/renene

Transient optimization of a new solar-wind multi-generation system for hydrogen production, desalination, clean electricity, heating, cooling, and energy storage using TRNSYS

Ali Dezhdar [a,b,1], Ehsanolah Assareh [c,e,*,1], Neha Agarwal [c,1], Ali bedakhanian [d], Sajjad Keykhah [e], Ghazaleh yeganeh fard [f], Narjes zadsar [f], Mona Aghajari [g], Moonyong Lee [c,**]

[a] Young Researchers and Elite Club, Dezful Branch, Islamic Azad University, Dezful, Iran
[b] Kimia Andimeshk Petrochemical Industries Company, Khuzestan, Iran
[c] School of Chemical Engineering, Yeungnam University, Gyeongsan, 38541, South Korea
[d] Faculty of Energy Engineering, Shahrood University of Technology, Shahrood, Iran
[e] Department of Mechanical Engineering, Dezful Branch, Islamic Azad University, Dezful, Iran
[f] Faculty of Mechanical Engineering, Alzahra University, Tehran, Iran
[g] Department of Architecture, Semnan Branch, Islamic Azad University, Semnan, Iran

ARTICLE INFO

Keywords:
Cooling
Heating
Clean electricity
Hydrogen production
Multi-generation system
Energy storage

ABSTRACT

In the current study, a renewable system with two potential wind and solar energies for electricity production, cooling, and heating has been investigated. The proposed system included reverse osmosis, heat pumps, fuel cell subsystems, wind turbines, photovoltaic/thermal panel units, battery storage, and a hydrogen storage tank. Given Iran's high potential for renewable energy, a performance analysis of six cities, Esfahan, Zanjan, Bandar Anzali, Ahvaz, Bandar Abbas, and Tabriz was done to determine where the proposed power plant should be located. Six decision factors were analyzed for system performance: solar panel angle, solar panel count, wind turbine count, cooling capacity, heating capacity, and fuel cell power. The findings demonstrate that the number of solar panels, wind turbines, and fuel cells significantly influences power, fuel consumption, and system costs. Finally, the outcomes were analyzed by the Response surface method to choose the best system that can satisfy the demand for residential units for one year. To evaluate the effectiveness of the suggested method, a 100-unit apartment building with a 196-square-meter floor space was considered. The results also showed that the combination of hydrogen units and battery storage reduced variations in supply and demand and correctly stabilized the stored energy during a drop in output. The suggested system has a life cycle cost of 674278.4$/h and the capacity to generate 225694.8 kWh of surplus power for residential units with a thermal comfort index. According to the optimization results, the system's optimal panel count was 106, the optimal angle was 26°, the optimal fuel cell power was 65.6 kW, the ideal wind turbine count was 24, the ideal heating capacity was 20.2 kW, and the optimal cooling capacity was 48.7 kW.

1. Introduction

One of the most important concerns facing the world right now is energy. Cleanliness, concern for the environment, safety, and affordability are crucial aspects of energy delivery. Multi-generation systems provide high-efficiency, low-cost, sustainable, and clean solutions to this issue [1]. The research that has been done on harnessing renewable energy for energy production is covered in the section that follows. Researchers have focused on solar energy as one of the most accessible renewable sources, but one of the drawbacks of solar energy is its instability. Solar energy is not always available, even on rainy days, so it is necessary to install energy storage sources to increase the stability of the system. In 2023, Shakibi et al. [2] carried out a case study to evaluate the effectiveness of the system with regard to climate change in the city of Las Vegas. They also carried out an economic research and

* Corresponding author. School of Chemical Engineering, Yeungnam University, Gyeongsan, 38541, South Korea.
** Corresponding author.
E-mail addresses: Ehsanolah.assareh@gmail.com (E. Assareh), mynlee@yu.ac.kr (M. Lee).
[1] These authors contributed equally to this article as the first authors.

https://doi.org/10.1016/j.renene.2023.03.019
Received 10 November 2022; Received in revised form 25 February 2023; Accepted 4 March 2023
Available online 9 March 2023

Nomenclature

A	area (m^2)
L	panel length
a	axial induction factor
AOC	system's operating cost during a year ($)
c	*specific heat capacity (J/kg.K)*
C_P	Power wind turbines coefficient
d	*discount rate*
EIR	energy efficiency
M	metabolic rate ($W.m^{-2}$)
f	ON/OFF statues of a component (0 or 1)
$T_{setpoint}$	*set-point temperature*
G_T	solar radiation ($kJ/hr.m^2$)
$\dot{m}$	*mass flow rate (kg/h)*
i	*inflation rate*
I	current (A)
I_C	initial investment cost ($)
L	length (m)
L_B	thermal load of inhabitants' body
n_f	number of factors
T	temperature (°C)
U	*voltage (V)*
$\dot{V}_{H_2}$	*total hydrogen consumption*
x	*factor*
y	*response*
n_t	number of timesteps
n_L	lifespan (year)
N_{tubes}	number of tubes in photovoltaic panel
Q_{gen}	heat produced by fuel cell
$\dot{q}_{sens}$	*sensible cooling performed by the heat pump (kJ/h)*
$\dot{q}_{tot}$	*heat pump cooling performed by the (kJ/h)*
$\dot{q}_{sens}$	*sensible cooling performed by the heat pump (kJ/h)*
$\dot{q}_{tot}$	*total cooling performed by the heat pump (kJ/h)*
$T_{f,out}$	*outlet temperature of the heat transfer fluid*
$E_{PV/T}$	*electricity produced by the photovoltaic panel*
v	wind speed
a	*axial induction factor*
$C_{P,max}$	*The maximum power coefficient*

Abbreviations

AFC	alkaline fuel cell
BFC	boiler fuel consumption
PMV	predicted mean vote
DOE	design of experiments
HP	heat pump
PV/T	photovoltaic/thermal
RSM	response surface methodology
WT	Wind turbine
LCC	life cycle cost
IAM	incidence angle modifier
EIR	The bypass fraction
OEC	overall electricity consumption
PWF	Present value factor

Scripts

a	air
amb	ambient
AS	*actual air state*
db	dry bulb
f	heat transfer fluid
in	inlet
out	outlet
r	Wind turbines rotor
set point	set point
wb	wet bulb
$\tau\alpha$	*photovoltaic panel transmittance-absorptance*

Greek symbols

ε_m	*emissivity*
ω	*absolute humidity ratio (kg_{water}/kg_{air})*
η	*efficiency*
$\tau\alpha$	*transmittance-absorptance product for photovoltaic panel*
v	*Wind speed (m/s)*
ρ_a	*Air density (kg/m^3)*
θ	*angle of incidence (°)*

multi-objective optimization of a solar and wind power plant. It was recommended to create more power using the many production systems under investigation, including the parabolic solar collector, wind turbine, thermoelectric generator, and their combination with the steam Rankine cycle. Additionally, a reverse osmosis desalination machine, a single effect absorption chiller, proton exchange membrane electrolysis, and cooling of hydrogen generation were employed to create fresh water. Based on an analysis of the first and second principles of thermodynamics and the performance of several thermal oils, Syltherm 800 oil was chosen as the optimum choice for use in a parabolic solar collector. In the second half, a model based on artificial neural networks was taken into consideration to rebuild thermodynamic difficulties. The best circumstances for the goal functions were discovered using the multimodal gray wolf optimization technique. The solar unit (901.4 kW) has the greatest exergy destruction value, according to the findings. This resulted in the city of Las Vegas producing 22.02 MWh of electricity and 4.50 tons of carbon dioxide in a year, resulting in an environmental cost of $107.8 annually in a case study that took into account the city's circumstances. In order to provide a Colombian power plant with the necessary energy in 2021, Lopez et al. [3] examined and contrasted the utilization of two different solar thermal collectors. A boiler's feed water was preheated using solar energy, which decreased the amount of fuel needed and energy lost in the power plant. Performance comparisons between a linear and parabolic solar collector were made. A PTC performed better, according to the findings of an energy assessment for two different kinds of solar collectors. One of the disadvantages of this study is the lack of energy storage for hours when solar energy is not accessible. Researchers like Dezhdar et al. [4], Assareh et al. and others have researched extensively in the area of mixing various components to produce various energies including electric energy, hydrogen, cooling, and heating. Energy, exergy, as well as the amount of exergy destruction in the system's units and components, as well as a thorough economic study of the system, were all performed. Finally, in these studies, focus was placed on the deployment of the researched system in various locations. In these two researches, by using renewable energies, including solar energy and ocean thermal energy, they produced vital products needed by humans. A hybrid energy system that employs solar energy to create electricity and fresh water will be optimized thermodynamically and economically for the city of Isfahan in 2022, according to Assareh et al. [5]. One of the major objectives of this system was to lower yearly expenses, and another aim was to boost efficiency. The components of this system were a concentrated solar power plant, a steam Rankine cycle, an organic Rankine cycle, a reverse osmosis unit, and a thermoelectric generator. Economic analysis of the system and exergy analysis were done to introduce the costs of the system components and the rate of exergy destruction of the system components. The results indicated that the solar unit has the highest cost due to the expensive equipment and on the other hand, it also has the highest rate of exergy destruction.

In order to meet the consumption load of a building in 2023, Nikbakht Naserabad et al. [6] constructed and assessed the performance of a hybrid energy system. The suggested system's schematic is shown in Fig. 15. In this article, four models were assessed to satisfy the demand load of a building in accordance with the limits of the cogeneration system in the off-design mode. Additionally, a comparison between the multi-generation structure and a conventional system was made to take into account government assistance policies in subsidizing energy carriers. Energy efficiency, relative net benefit of current value, and net benefit of future value of the proposed plan were the assessment criteria used in this study. According to the findings, thermal load has the greatest energy and exergy efficiency at 55.33 and 31%, respectively. Additionally, the relative net earnings in the present and future are $164,800 and $1.09 million, respectively. For the peak load pattern, the biggest relative net current and future value increases are $330,140 and $2.18 million. The findings indicated that the thermal load patterns and peak consumption load are the cogeneration system's optimum technical and economical alternatives, respectively. The peak load pattern also produced the best investment choice, which had a rate of return of 37.9% and a payback time of 4.25 years on the original expenditure. The multi-objective optimization of a biomass-based system for the generation of electricity and desalinated water utilizing the gray wolf optimizer and artificial neural network was addressed by Musharavati et al., in 2022 [7]. In this study, a biomass-based energy system that produces both power and fresh water was suggested. The gasifier, the compressor, the heat exchanger, the gas turbine, the combustion chamber, and the multi-effect desalination unit with thermal vapor compression are the primary parts of this power plant. The suggested system underwent a thorough thermodynamic and thermoeconomic study. In order to ascertain the impact of initial decision factors on system performance, a parametric analysis was also carried out. To find the best solution with the maximum energy efficiency and lowest overall cost, multi-objective optimization was used using the multi-objective gray wolf optimizer algorithm. In order to shorten computation time and quicken optimization, the artificial neural network served as a middleman in the process. In order to identify the energy system's optimum point, neural networks have been used to study the link between the objective function and the choice factors. The findings indicated that the ideal point's fresh water and power production rates are respectively 5127 kW and 38.6 kg/s. Additionally, it is determined that the ideal energy efficiency and total cost rate are 15.61% and 206.78 dollars per hour, respectively. The results also shown that the number of desalination units used had no impact on carbon dioxide emissions. Additionally, the air compressor pressure ratio is not a sensible variable, as seen by the dispersion distribution of the primary decision variable, and its ideal points are distributed across the whole range. The lack of energy storage technology, the inability to produce this system sustainably, and the impossibility of installing this system in diverse places are some of the drawbacks of this study. Siddiqui and Dincer [8] conducted an analysis of an energy system in 2019 that employs ammonia as a form of energy storage and hydrogen and fresh water production from solar and wind energy. In the first stage, power was produced using solar towers. The LCOE for this power generation ranged from 0.16 to 0.27 dollars per kWh. Additionally, the LCOE comparable to 0.037–0.048 $/kWh was computed for energy generation based on wind turbines. The SOFC system's LCOE ranged from 0.109 to 0.137 USD/kWh. They also employed a RO seawater desalination system in their research. The LCOE of this fresh water production technology ranged from 0.5 to 1.2 dollars per cubic meter. Similar to that, the price per kilogram of ammonia generated from hydrogen produced using PEM electrolysis ranged from 1.078 to 2.392 dollars. According to the findings, the total energy efficiency ranged from 48.1% to 53.3%. Additionally, during the year, Toronto's total energy efficiency ranged between 34.1% and 41.5%. A multi-objective optimization of a concentrated solar power plant for the generation of clean electricity, cooling, and freshwater for Turkey in 2020 was carried out by Gnaifaid et al. [9]. Solar radiation absorption was accomplished using parabolic collectors. A Rankine cycle turbine was utilized to generate power from the sun's heat, and an absorption chiller was used to generate cold. The reverse osmosis desalination system was started in part with the help of the produced electricity. Exergy effectiveness and system cost rate ranged from 14 to 9% and 33 to 287 dollars per hour, respectively. A 2020 energy analysis and economic optimization of solar energy systems and heat pumps with storage technologies for heating and cooling in residential buildings was carried out by Pinamonti et al. [10]. The goal of this study was to maximize the system's production capacity and decrease its reported cost rate. One drawback of this research is that it only looked at a building's analysis in terms of cooling and heating requirements; the research did not look at the building's power requirements. In order to produce hydrogen, Yüksel [11] studied the thermodynamics of a modified organic Rankine cycle combined with a parabolic collector in 2018. Solar energy was transformed into thermal energy using a parabolic collector, and the thermal energy produced in the modified ORC was utilized to produce electricity. Hydrogen was then created using the power. The analysis's findings indicated that one of the most significant elements impacting the system's energy efficiency and hydrogen generation rate was sun radiation. The system's energy efficiency rose from 58% to 64% when solar radiation climbed from 400 W/m2 to 1000 W/m2, and the rate at which hydrogen was produced grew from 0.1016 kg/h to 0.1028 kg/h. Assareh et al. [12] discussed the techno-economic study of the renewable system in 2022. This research looked at the technical and financial aspects of designing a cooling, heating, and combining power system from different renewable energy sources to satisfy the demands of an apartment complex. Trnsys software was used to model the suggested system, and after that, the target functions were improved to boost the system's performance. The primary parts of this system are the heat pump battery, wind turbine unit, and solar unit. Assareh et al. [13] studied a case study of climate change in Australia, Spain, South Korea, and Iran in 2023 and looked into a renewable system based on solar energy to create electricity and fresh water from a new gas power plant and a solar power plant. This research looked at a novel power plant cycle that included integrating a solar power plant into a Brayton cycle before the combustion chamber. This research looked at how the suggested system would respond to radiation, wind speed, and ambient temperature in four distinct countries. The most significant and useful characteristics in this research are the efficiency of the gas turbine, intake temperature of the turbine, inlet pressure to the steam turbine, and inlet temperature to the gas turbine. The combustion chamber, heliostat, solar receiver, multi-effect desalination, gas turbine 1, and thermoelectric each contribute the most to exergy destruction, according to the system's exergy analysis. This cycle's total output power was 190.7 MW, while its overall energy losses were calculated to be 47.73 MWh. The compressor and gas turbine 1 in the proposed cycle have, respectively, the highest cost rates, and the cost rate of the energy produced by the proposed system is 2288 dollars per hour, according to the system's economic analysis. Their research showed that cycling performed best in the local weather in Busan, Melbourne, Barcelona, and Bandar Abbas. A hydrogen generation system based on solar energy and chemical energy storage using ammonia was the focus of Chen et al. [14] research in 2021. The article provides a unique approach for power production combining ammonia-based chemical thermal energy storage and high-temperature water electrolysis (using a solid oxide electrolyzer cell). A novel system with ammonia-based energy storage, Brayton cycle, electrolyzer, and solar panel subsystems was examined. Behzadi et al. (2019) [15] proposed a unique solar cycle to generate energy and hydrogen. A genetic algorithm was used to carry out the optimization. Condensers were replaced with thermoelectric machinery to improve energy efficiency, boost electricity output, boost hydrogen synthesis, and lower cycle costs. The research's conclusions indicated that the suggested thermoelectric cycle had a greater energy efficiency, a higher rate of hydrogen generation, and a lower overall cost rate. Energy efficiency and total cost rate for the proposed system were 12.12% and

0.1762 dollars per hour, respectively. Ozturk and Dincer [16] developed and analyzed a green hybrid hydrogen generating system in 2022. In this research, an integrated system based on solar energy, ocean waves, and wind energy to manufacture renewable (green) hydrogen and mix it with natural gas possibly accessible in the Black Sea was built and analyzed, as well as a case study for the Turkish city of Zongaldek. To use natural gas supplies in a more effective and ecologically responsible manner, this research focuses on mixing it with 20% volumetric hydrogen. To this end, the hydrogen generation capability from renewable energy sources such as wind, sun, and waves was determined to be 1432 kg, 174220 kg, and 1257 kg, respectively. Using a neural-genetic network algorithm, Izadi et al. [17] designed and optimized hospital rooms to create oxygen and power using solar photovoltaic panels with hydrogen storage systems in 2023. According to this study, the Covid-19 illness has influenced energy consumption and production patterns in rural and urban sectors across many industries. As a result, energy demand has increased; consequently, the majority of healthcare facilities report energy shortages, particularly in the summer; therefore, the integration of renewable energy in hospitals is a promising method that can reliably generate electricity demand and emit less carbon dioxide. This article simulates a hybrid renewable energy system with hydrogen energy storage to meet the energy requirements of hospital wards and wards caring for Covid-19 patients. The created oxygen is extracted from the hydrogen storage system and stored in medicinal capsules to supply patients with the oxygen they need. The data indicated that the Covid-19 sector accounts for 29.64% of the yearly energy usage. After optimizing the modeled system using a neural network genetic algorithm, the ideal quantity of network power demand, carbon dioxide emission, oxygen capsules, and cost rate were calculated. With 976 photovoltaic panels, a 179 kW fuel cell, and a 171.2 kW electrolyzer, the yearly carbon dioxide emission is estimated to be 315.8 tons, and 67,833 filled medicinal oxygen capsules may be produced. For the stated system design, the cost and power consumption from the grid are 469.07 MWh per year and 18.930 Euros per hour, respectively. In 2022, Assareh et al. [18] investigated the thermodynamics and economics of a multi-energy production system for the generation of electricity and fresh water that employed solar concentrators, compressed air energy storage units, and multi-effect desalination. Heliostat, gas turbine, multi-effect desalination, and compressed air energy storage subsystems were among the system's components. The system's economic study revealed that the compressed air storage source unit, solar unit, and gas turbine have the greatest prices among system components, while the heliostat, receiver, and gas turbine had the highest exergy destruction rates. The results demonstrated that this system performed at its maximal efficiency under Esfahan's climatic circumstances. An energy and economic assessment and optimization of a power generating system combining solar, wind, and ocean thermal energy for the city of Bandar Abbas, Iran, was carried out in 2021 by Assareh et al. [19]. The solar thermal collector, organic Rankine cycle, and wind turbine subsystems make up this system. This system uses an organic Rankine cycle turbine to generate power, which is then transformed into electrical energy and sent to the country's electrical distribution network. In its ideal form, this system is capable of generating 448 kW of electricity. Additionally, the system's energy efficiency was 13.88%. The employment of thermoelectric in the organic Rankine cycle increases the system's production capacity, according to the study's findings. In the area of utilizing renewable energies to create various forms of energy, several kinds of study have been carried out [1–19], however in these systems, more focus has been placed on using one type of renewable energy, such solar or geothermal energy, and less on using others. Simultaneous energy is thought to improve the system's stability. because energy sources like solar energy are not constant and lower the system's stability. Additionally, none of the aforementioned studies have explored the use of battery and hydrogen sources to store extra energy and utilize it during periods of high consumption as well as during times when renewable energy sources are not accessible. The system's performance has been improved in the present study using both solar-wind energy and energy storage sources. Because the primary objective of many renewable energy production systems is to meet human needs for energy, such as electricity, cooling, and heating, and in all of the aforementioned studies, the performance of the system has not been examined in relation to the energy supply required by buildings or residential units. The study necessary to supply the load of the building was not done; the research simply looked at how much energy the system generated. We came to the conclusion that the simultaneous use of various renewable energy sources, modeling, optimization, economic analysis, and long-term analysis of these systems are highly significant based on the study done and the worldwide need to utilize more clean energy. In the current work, a wind and solar energy integrated hybrid system was modeled. This system yearly provided 100 residential units with energy, hot water, cooling, heating, and fresh water. A strategy to construct and improve renewable energy systems for six cities was suggested, taking into account Iran's capacity to utilize renewable energy. Solar panels, wind turbines, fuel cells, battery storage banks, heat pumps, and reverse osmosis are the system's primary subsystems. Zanjan was chosen as the top city based on system performance, power generation, and economic analyses of each of the six cities. Parametric studies were carried out in order to explore the effects of various factors and identify the affecting parameters, and statistical techniques were used to choose the best mode. For parametric analysis and multi-objective optimization, six decision variables—solar panel angle, wind turbine count, fuel cell capacity, heat pump cooling and heating capacities, and solar panel count—were taken into account. TRNSYS software was used to examine system modeling and analysis. This study's investigation of system performance focused on four key goals: total electricity use, boiler fuel use, life cycle cost, and average rating as a gauge of thermal comfort. The simultaneous use of two renewable energies may be the key breakthrough of this study. the use of energy storage devices, as well as a case study, parametric analysis, multi-objective optimization, and economic and technical evaluation of the suggested cycle.

The purpose of this study can be presented as follows.

- Obtaining a hybrid system due to solar and wind energy to increase the technical performance of the system.
- Applying energy storage resources to store energy and to meet requirements during peak consumption.
- Surveying the changes in design parameters on system performance. Studying the climate changes of multiple regions in the country on the suggested system.
- Finding the best region in Iran to launch the recommended system.
- Multi-objective optimization to find the best value for the objective functions and decision variables.
- Checking the supply of required loads of a residential building by the suggested system.

The novelty of this study may be summed up as the simultaneous use of two clean energy sources, clean solar and wind energy, as well as the use of two energy storage sources to improve system performance and satisfy the demands of a residential building at peak load and peak consumption. The instability of renewable sources throughout the day makes it a vital problem that need to be taken into account in subsequent study. Additionally, this study addresses the construction of a multi-energy production system to fulfill the demands of a residential complex and remove the need for power, cooling, and heating. The proposed system can supply the necessary load for a 100-unit building, according to the research. It is also demonstrated that using renewable solar and wind energy simultaneously will improve the system's performance. The impact of environmental parameters in various regions of Iran on the system's performance is also examined.

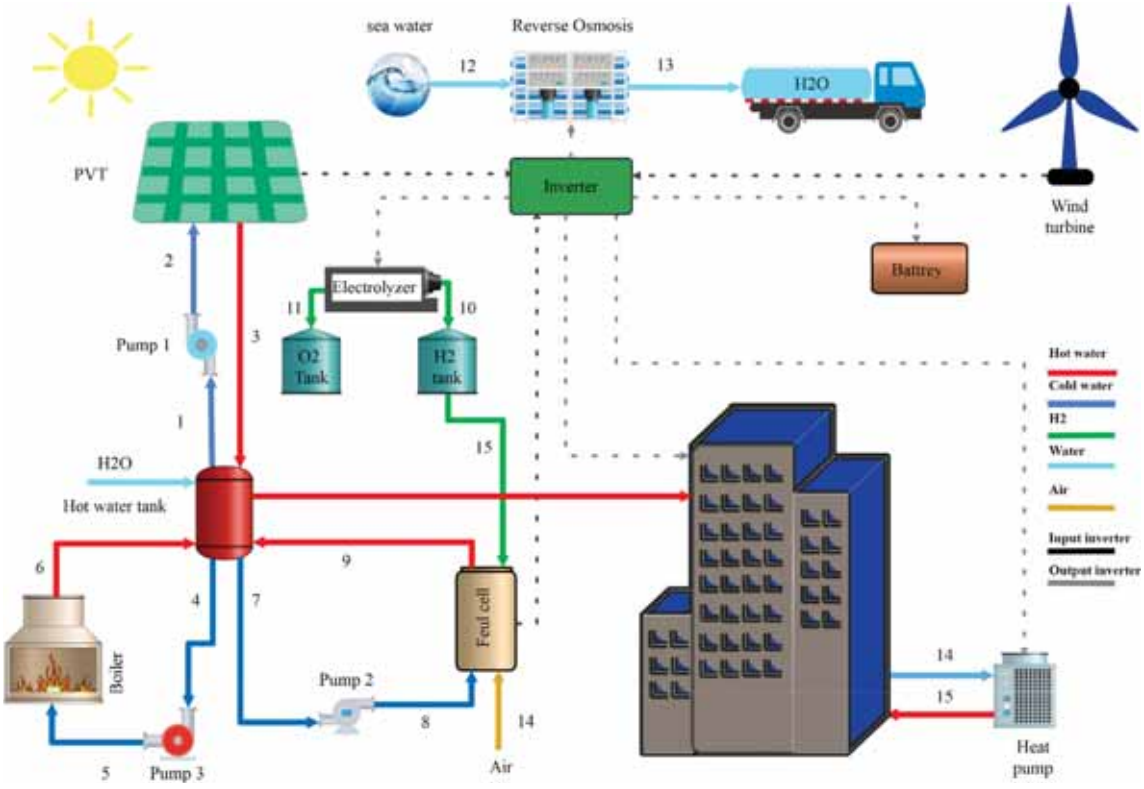

Fig. 1. Proposed system.

2. System description

The analyzed system's schematic is shown in Fig. 1. The system uses wind and solar energy to operate. The system consists of photovoltaic panels, which absorb solar energy and produce electricity, wind turbines, heat pumps, which provide cooling and heating, PEM electrolysis, which produces hydrogen, and reverse osmosis, which produces fresh water. In this system, water is introduced into the PV/T circuit's Photovoltaic panel tubes, where the heat from the sun's radiation raises the water's temperature. The hot water is then transferred to the hot water tank, raising the water's temperature and lowering the photovoltaic panel's cell temperature at the same time, increasing the efficiency of electricity production. Three hot water inlets and three cold water outlets can be found on the hot water storage tank. There is an exit for each input until the temperature of the tank spa is dropped and the tank is warmed using the sun panels, fuel cell, and backup boiler. The spa entrances receive the spa water from the solar panels, fuel cell, and backup boiler. Obtain the inside of the building's required temperature for consumption. The wind turbines assist solar panels in generating system power by supplying electricity for the building, electrolyzer, and reverse osmosis. A further component of the system is the fuel cell, which aids the solar cells in producing hot water when the sun isn't shining, as well as powering the system. The HP is in charge of supplying the target buildings with heating and cooling. It supplies the necessary

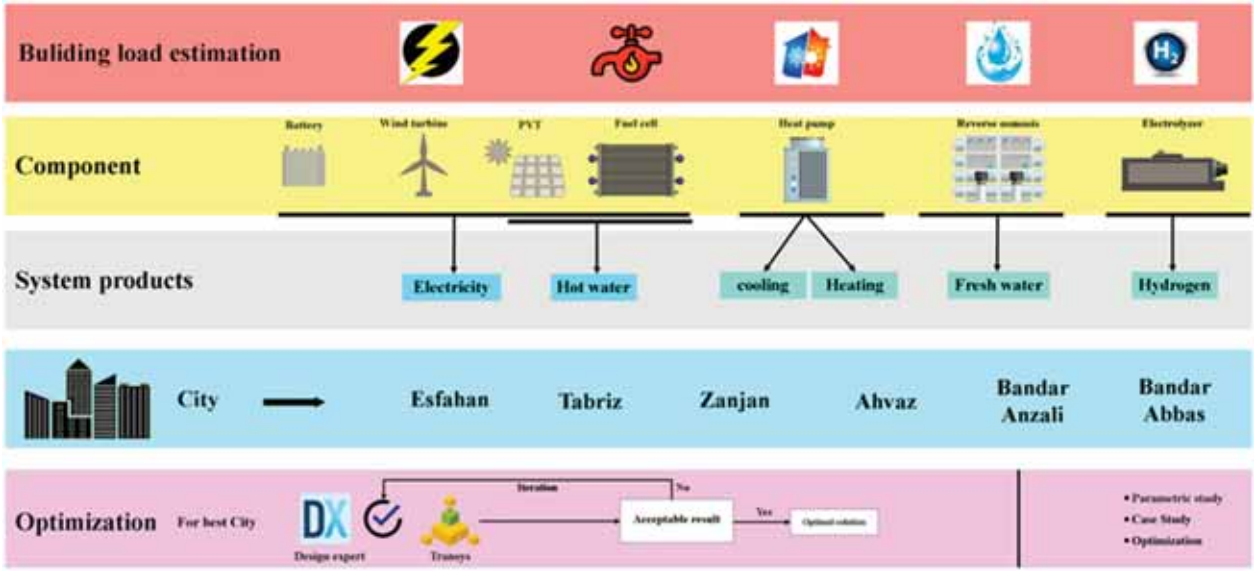

Fig. 2. System methodology.

Table 1
Specifications of each apartment unit.

Item	Value	unit	Reference
Area of each unit	*196*	m^2	[29]
Window area	*3*	m^2	[30]
Number of people per unit	*4*	*(−)*	[30]
Heat transfer in the floor	*0.319*	$W.m^{-2}.K^{-1}$	[31]
heat transfer in the windows	*3.11*	$W.m^{-2}.K^{-1}$	[31]
heat transfer coefficient of the walls	*0.510*	$W.m^{-2}.K^{-1}$	[31]
heat transfer coefficient of roof	*0.316*	$W.m^{-2}.K^{-1}$	[31]
Absorption of solar radiation from the roof	*0.61*	*(−)*	[32]
Radiation absorption of building walls	*0.61*	*(−)*	[32]
The number of windows	*4*	*(−)*	[33]
Ceiling height of each unit	*2.8*	*m*	[33]
The total number of people in the building	*400*	*(−)*	-

heating and cooling according to the needed temperature for each structure, and the HP gets its energy from the system's power output. As previously noted, reverse osmosis, which is in charge of delivering fresh water to the system, uses a portion of the manufacturing power generated by wind turbines.

The following assumptions are shown to simplify the problem solving.

- Pumps are isentropic.
- The pressure drop in pipelines is negligible.
- In this research, it was proposed that the potential and kinetic energy changes are very small, and for this reason, its calculation was deleted.

Fig. 2 displays the design process, the solution approach, and the system's products and components. This method aims to satisfy the requirements of the residential complexes while producing clean goods and reducing environmental damage.

In this system, the need for a multiple production system for exploitation is satisfied by the use of two clean, readily available renewable energies, including solar energy and wind energy. An energy storage source has been employed to keep the system running constantly, provide the needed energy during peak hours, and improve system dependability.

2.1. Modeling of the system

TRNSYS software is used to simulate the proposed system in this study. For the sake of this modeling study, this program includes comprehensive libraries of system and technology components, including several kinds of solar systems, buildings and heating-cooling loads, wind energy, etc. The TRNSYS library has been completely verified by earlier experimental studies [20–27] and is used for predictive system modeling [28].

2.1.1. Building

In this study, two buildings with 12 and 13 stories, respectively, and a total of four units on each level, are taken into consideration to evaluate the performance of the suggested system in terms of addressing the demands of residential buildings. According to Refs. [20,29], each unit is 196 square meters. The characteristics listed in Table 1 to introduce these features are present in this building.

The quantity of hot water used by the planned structure is shown hourly over the course of the year in Fig. 3a. Additionally, the quantity of electrical energy used by the planned structure is shown hourly in Fig. 3b [34]. Trnsys software has estimated the data required to determine the building's energy usage depending on the weather in Zanjan, Iran.

Fig. 4 depicts changes in the city of Zanjan's ambient temperature and relative humidity over the course of a year (8760 h). As is common knowledge, the summer months have the greatest average temperature, while the winter months have the lowest average temperature. The outcome also reveals that the seasons with the greatest and lowest relative humidity are winter and spring, respectively.

Fig. 5 shows the estimated changes in the analyzed building's cooling and heating energy usage over the course of a year and hourly for the city of Zanjan. The findings indicate that although cooling energy usage rises throughout the summer, heating demand rises during the colder winter and fall months.

2.1.2. PV/T

The photovoltaic panel generates electricity and absorbs heat energy using the tubes that circulate the fluid on the back of the device. The output temperature of the heat transfer fluid and the amount of energy produced by the solar panel were calculated using equations (1) and (2) [35].

$$E_{PV/T} = (\tau\alpha)_n \cdot IAM \cdot G_T \cdot A \cdot \eta_{PV/T} \tag{1}$$

$$T_{f,out} = \left(T_{f,in} + \frac{\varepsilon_m}{\kappa}\right)\exp\left(\frac{N_{tubes}}{\dot{m}_f c_f}\frac{\kappa}{\theta}L\right) - \frac{\varepsilon_m}{\kappa} \tag{2}$$

Where $\tau\alpha$ is the photovoltaic panel transmittance-absorption product, IAM is the incidence angle modifier, G_T is the general solar radiation incidence of the photovoltaic panel, A is the collector area, and $\eta_{PV/T}$ shows the collector nominal efficiency. ε_m is the emissivity, L indicates the collector length, and θ is the incidence angle.

2.1.3. Wind turbine

Type 90 was utilized to model the wind turbine, in which the production power of the wind turbine is computed based on the Betz theory, which is given in equation. (3) [36]:

$$E_{WT} = \rho_a C_P A_r v^3; C_P = 4a(1-a)^2 \tag{3}$$

Where ρ_a is the air density, A_r shows the area of the Wind turbine rotor, v is the wind speed, C_P is the power coefficient of the Wind turbine, and a is the axial induction factor. The maximum power coefficient, $C_{P,\max}$, was 59.3% and is known as Betz's limit.

2.1.4. Heat pump

To model the heat flow, the heat pump type 966 from the library was applied, which computes four coefficients for cooling mode and two coefficients for heating mode for bypass fraction, total current cooling/heating capacity, reasonable cooling/heating capacity.

Moreover, EIR is defined as the fraction of power supplied to the rated capacity of unit while operating under rated conditions [37]. The coefficients applied in the cooling and heating modes are expressed in equations (4) and (5), respectively [38].

$$\begin{cases} f_{totCool} = tc_1 + tc_2 T_{wb,in} + tc_3 T_{wb,in}^2 + tc_4 T_{db,amb} + tc_5 T_{db,amb}^2 + tc_6 T_{wb,in} T_{db,amb} \\ f_{sensCool} = sc_1 + sc_2 T_{wb,in} + sc_3 T_{wb,in}^2 + sc_4 T_{db,amb} + sc_5 T_{db,amb}^2 + sc_6 T_{wb,in} T_{db,amb} \\ f_{EIR,c} = cp_1 + cp_2 T_{wb,in} + cp_3 T_{wb,in}^2 + cp_4 T_{db,amb} + cp_5 T_{db,amb}^2 + cp_6 T_{wb,in} T_{db,amb} \\ f_{Bypass} = bf_1 + bf_2 T_{wb,in} + bf_3 T_{wb,in}^2 + bf_4 T_{db,amb} + bf_5 T_{db,amb}^2 + bf_6 T_{wb,in} T_{db,amb} \end{cases} \tag{4}$$

$$\begin{cases} f_{heat} = th_1 + th_2 T_{wb,in} + th_3 T_{wb,in}^2 + th_4 T_{db,amb} + th_5 T_{db,amb}^2 + th_6 T_{wb,in} T_{db,amb} \\ f_{EIR,h} = hp_1 + hp_2 T_{wb,in} + hp_3 T_{wb,in}^2 + hp_4 T_{db,amb} + hp_5 T_{db,amb}^2 + hp_6 T_{wb,in} T_{db,amb} \end{cases} \tag{5}$$

Bypass fraction, EIR, capacity and reasonable capacity were provided after computing all coefficients by multiplying the nominal value of every parameter with the corresponding coefficient. The enthalpy and temperature of the air coming out of coil is analyzed applying equation (6). When the situations at the coil air outlet are specified, the coil air is mixed with the bypass air, as indicated in Eq. (7).

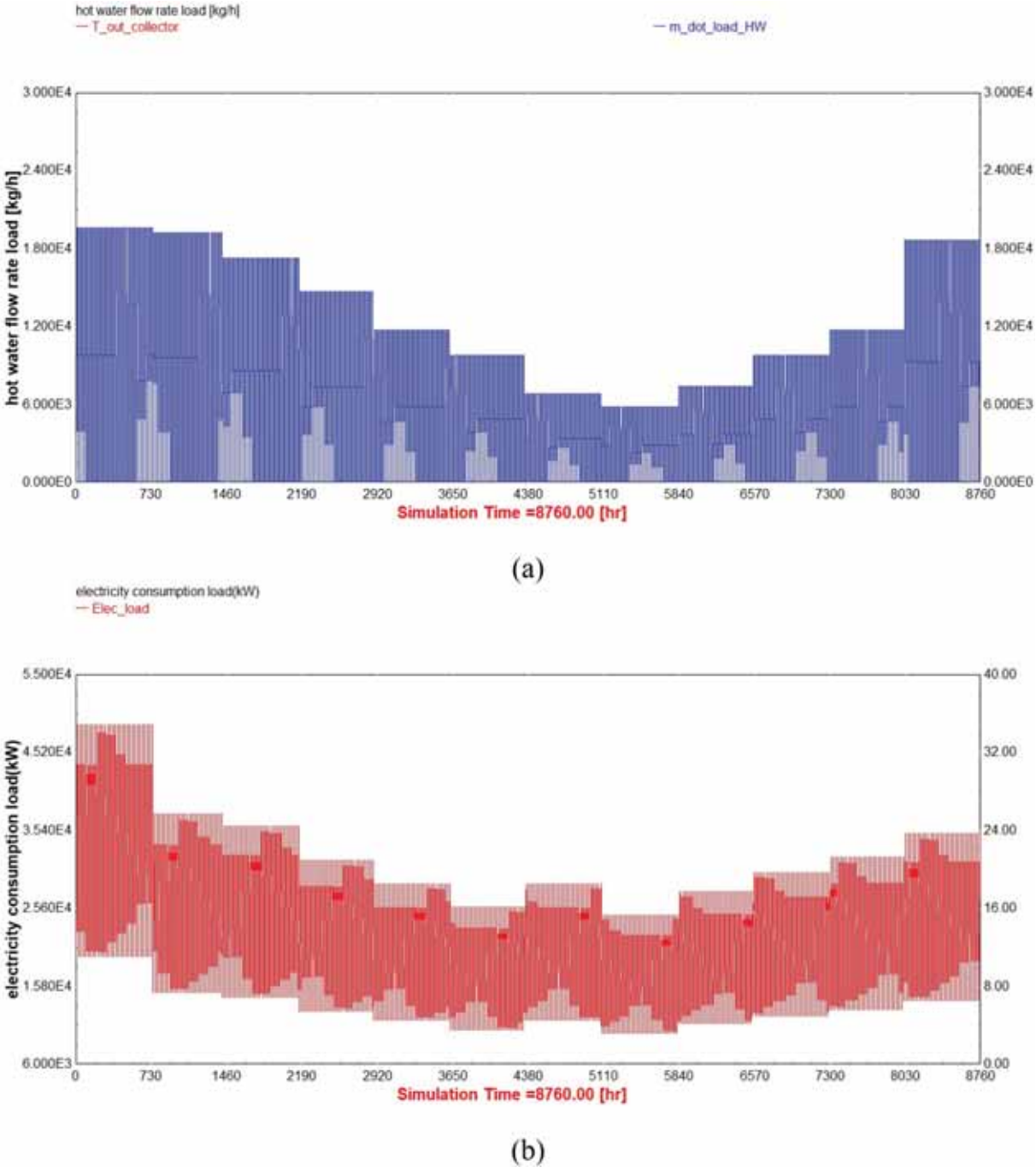

Fig. 3. Hourly building energy consumption throughout the year (a) Hot water consumption. (b) amount of electricity consumption.

$$\begin{cases} h_{coilOut} = h_{airIn} - \dfrac{\dot{q}_{tot}}{\dot{m}_{air}\left(1 - f_{bypass}\right)} \\ T_{coilOut} = T_{dbIn} - \dfrac{\dot{q}_{sens}}{\dot{m}_{air}C_{air}\left(1 - f_{bypass}\right)} \end{cases} \tag{6}$$

$$\begin{cases} h_{airOut} = f_{bypass}h_{airIn} + \left(1 - f_{bypass}\right)h_{coilOut} \\ \omega_{airOut} = f_{bypass}\omega_{airIn} + \left(1 - f_{bypass}\right)\omega_{coilOut} \end{cases} \tag{7}$$

2.1.5. Fuel cell unit

Alkaline fuel cell is mathematically modeled applying type 173. (8–10), while the stack output power was provided from Eq. (11) [39]. Besides, the energy efficiency of the fuel cell was computed applying the cell voltage, hydrogen enthalpy at standard conditions, Faraday's constant and number of electrons, as indicated in Eq. (12) [40]. The consumption of hydrogen and the total heat of the fuel cell were computed utilizing equation. (13) and (14), respectively [39].

$$U_{cell} = \frac{U_{mod}}{n_{c,ser}} \tag{8}$$

$$U_{mod} = U_0 - b\log\left(I_{stack}\right) - R_{ohm}I_{stack} \tag{9}$$

$$U_{stack} = n_{m,ser}U_{mod} \tag{10}$$

$$E_{stack} = U_{stack}I_{stack} \tag{11}$$

$$\eta_E = \frac{U_{cell}.n_e.F}{\Delta_{H_2}} \tag{12}$$

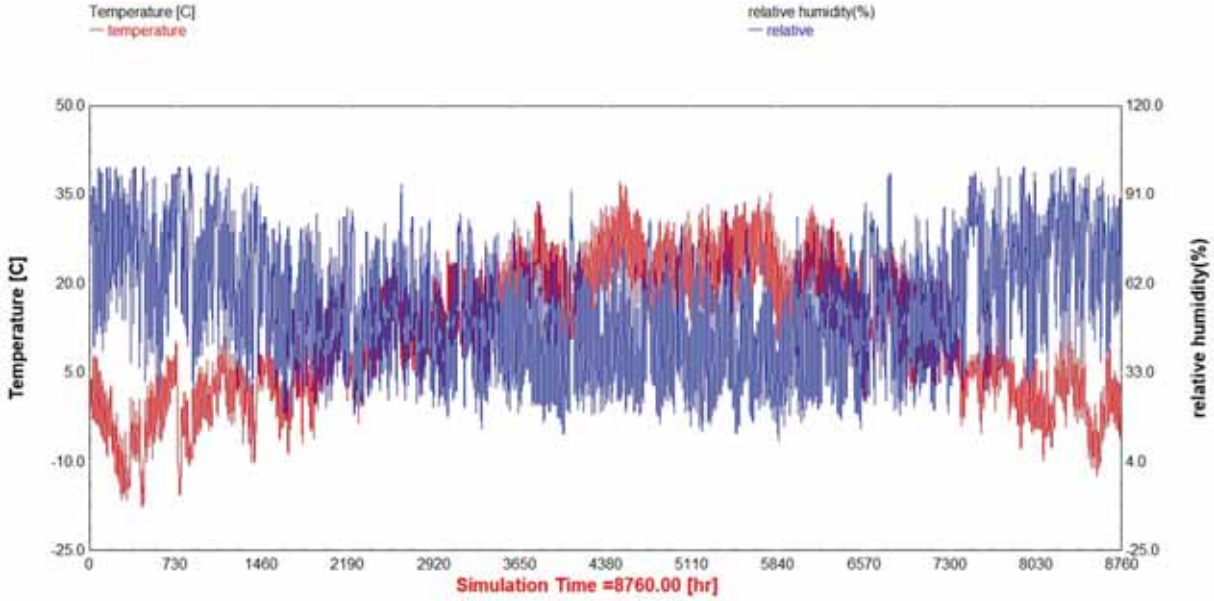

Fig. 4. Hourly changes in ambient temperature and relative humidity in Zanjan city all through the year.

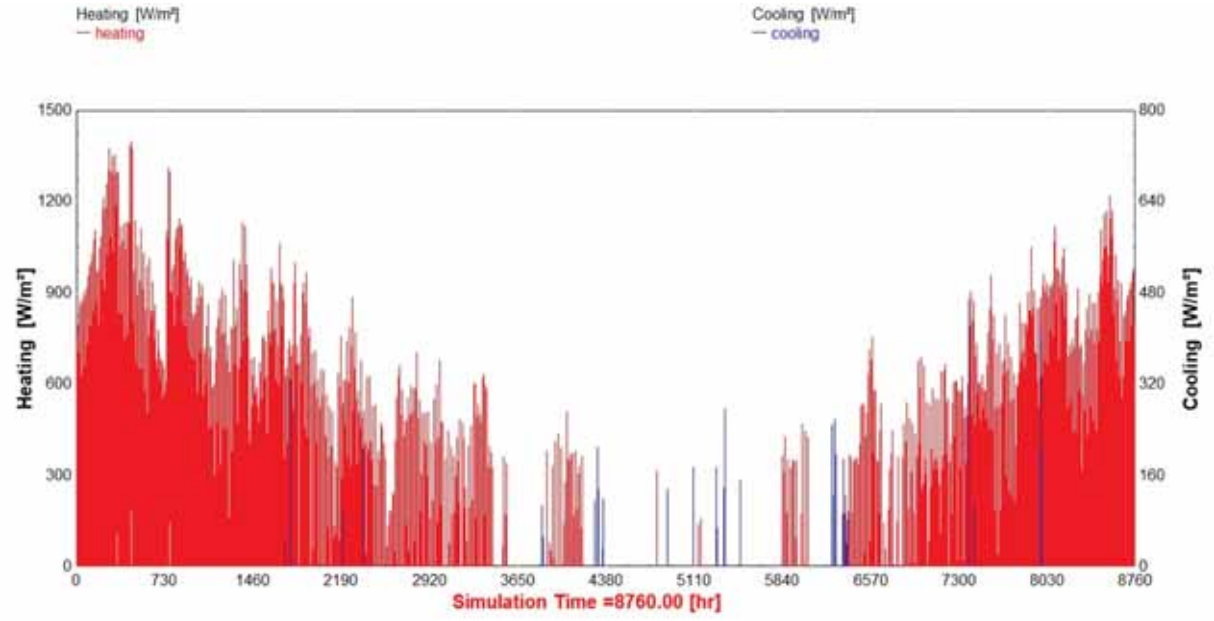

Fig. 5. The cooling and heating energy consumption of the study building.

$$\dot{V}_{H_2} = \frac{n_{c,ser} n_{m,ser} I_{FC}}{zF\rho_{gas}} S_{H_2} \eta_F \tag{13}$$

$$Q_{gen} = E_{stack}\left(\frac{1-\eta_E}{\eta_E}\right) \tag{14}$$

2.1.6. Electrolyzer unit

Electrolyzer analysis is controlled by thermodynamic analysis and heat transfer principles. The overall hydrogen production rate of the electrolyzer, which is identified by the number of cells connected in series, can be computed from Equation (15) [38–42]:

$$\dot{n}_{H_2} = \eta_f N_{cells} \frac{I_{ely}}{nF} \tag{15}$$

2.1.7. Reverse osmosis unit

The output power of the steam cycle pump was computed applying equation (16) [43,44,and 45]:

$$PumpPower = \dot{W}_{net} \times 1.79 \tag{16}$$

Freshwater rate was provided from equation (17):

$$Fresh\ Water\ Rate = p1 \times PumpPower^2 + p2 \times PumpPower + p3) \Big/ (PumpPower + q1) \tag{17}$$

The unit of freshwater production rate in this research is cubic meters per hour.

The coefficients due to the equation of 17 are listed in Table 2.

The initial input variables for modeling and solving the suggested system are shown in Table 3. The tariff for the purchase of natural gas as well as the purchase price and sale price of electricity have all been taken into account in the calculations, according to the reports presented [46].

Table 2
Fresh water rate relationship coefficients.

Coefficients	value
p1	*0.06739*
p2	*183.2*
p3	*130.2*
q1	*867.3*

Table 3
Input data to model and solve the proposed system.

Item	Parameter	Value	unit	Reference
Wind turbine	*rated power*	*100*	*kW*	[47]
	hub height	*40*	*m*	[47]
	Model	*2019 COE DW 100*	*(−)*	[47]
Boiler	*Fuel*	*Natural gas*	*(−)*	[31]
	combustion efficiency	*0.87*	*(−)*	[31]
	set point temperature	*65*	*°C*	[31]
photovoltaic panel	*Dimension*	*1.658 × 0.992*	*m*	[48]
	bond thermal conductivity	*45*	*$W.m^{-1}.K^{-1}$*	[48]
	Slope	*33*	*°*	[41]
Alkaline fuel cell	*electrode area*	*100*	*cm^2*	[49]
	number of fuel cell modules in series per stack	*64*	*(−)*	[49]
Hot water tank	*Volume*	*16.5*	*m^3*	[37]
Electrolyzer	*electrode area*	*0.25*	*m^2*	[49]
	number of cells is series	*70*	*(−)*	[49]
	number of stacks in parallel	*3*	*(−)*	[49]
	thermal resistance	*0.0563*	*K/W*	[49]
Lifetime	*System lifespan*	*25*	*years*	[31]
Compressed gas tank	*maximum pressure*	*400*	*bar*	[49]
	Volume	*50*	*m^3*	[49]
Battery	*Type*	*Lead Acid*	*(−)*	[49]
	number of cells in series	*110*	*(−)*	[49]
	nominal battery storage capacity	690 Ah	*(−)*	[49]
Heat pump	*bypass fraction*	*0.1148*	*(−)*	[46]
	cooling energy input ratio	*0.256*	*(−)*	[46]
Electricity	*purchase price*	*0.02*	*$/kWh*	[50]
	sale price	*0.046*	*$/kWh*	[50]
Natural gas	*purchase price*	*0.03*	*$/$m^3$*	[50]

2.1.8. Response surface method

The response procedure method, sometimes referred to as the RSM response surface method, is regarded as one of the techniques for experimental modeling and design. Numerous phenomena are modeled in engineering sciences based on their own theories. This is in contrast to the reality that many events cannot be well described mathematically because of the abundance of controlling variables, the lack of recognized mechanisms, or the complexity of the computing process. The use of experimental modeling techniques is efficient in these circumstances; one such technique is the response procedure approach.

The optimization study applying RSM can be divided into six steps as follows.

- Selection of independent variables from major impacts on the system via screening studies and delimitation of the test area, based on the purpose of the study and the experience of the researcher.
- Selecting the test plan and conducting tests based on selected test field
- Mathematical statistical analysis of experimental data provided via proper polynomial function
- Suitability evaluation
- Confirming the requirement and possibility of moving to the desired area
- Providing optimal values for each studied variable

Table 4
Range of decision variables.

Design variables	lower bound	upper bound
Number of Photovoltaic panel (−)	*0*	*300*
Number of wind turbines (−)	*0*	*20*
Power fuel cell (kW)	*0*	*100*
Heat pump cooling capacity (kW)	*0*	*80*
Heat pump heating capacity (kW)	*0*	*80*
Photovoltaic panel angle (o)	*0*	*90*

This optimization technique looks at how factors affect responses in order to get the best possible mix of variables [51]. The fundamental benefit of the response surface method optimization approach over other optimization methods is that it requires less simulation instances overall, resulting in a softer and more organized analysis of the components, their interactions, and the simulation of certain responses [52]. Applying CCD, the general second order RSM model is expressed in Eq. (18)

$$y = r_0 + \sum_{i=1}^{n_f} r_i x_i + \sum_{i=1}^{n_f} r_{ii} x_i^2 + \sum_{i<j=2} \sum^{n_f} r_{ij} x_i x_j \tag{18}$$

where y shows the chosen response, x is the factor, n_f is the number of factors and r represents the model coefficients provided from the regression analysis. The response surface approach is used to optimize the renewable system depending on the current work. Six design parameters—introduced in Table 4—that are regarded as having the greatest influence on system performance were taken into account as choice factors. The entire amount of power produced by the system and its capital expenses are directly impacted by the quantity of solar panels and wind turbines, as well as other factors. The creation of electricity, thermal energy storage, and the quantity of hydrogen produced, used, and stored all affect the fuel cell unit's capacity. The job of maintaining the thermal comfort of the building is performed by heat pumps. The decision-making variables' upper and lower bounds are defined in Table 4. RSM and CCD delivered 52 simulation runs based on the goal functions, the quantity of decision variables, and their fluctuation ranges. In order to solve the optimization process and use the RSM approach to enhance the system's technical and financial performance, Design-Expert software [53] was employed.

Four objective functions—total electricity consumption, boiler fuel consumption, anticipated average vote, and life cycle cost—have been chosen in order to optimize.

The overall amount of electricity used It indicates the difference between the total power production and total power consumption, which are computed using the relation, and the load profile of the building. (19).

$$OEC = \frac{\sum_{i=1}^{n_t} \left(E_{loadprofile} + E_{HP} + E_{elctrolyzer} + E_{pumps} + E_{compressor} - E_{PV/T} - E_{fuelcell} - E_{WTs} \right)}{3600 \times \frac{1}{Dt}} \tag{19}$$

Table 5
Objective functions.

Name	Objective
Overall electricity consumption	*Minimize (kWh/year)*
Boiler fuel consumption	*Minimize (m3/year)*
Predicted mean vote	*target = 0 (−)*
Life cycle cost	*Minimize ($)*

Table 6
Validation of water softener with the research of Nafey and Sharaf [55].

Variable	Present study	Nafey and Sharaf [55]	Unit	Difference (%)
$\dot{W}_{pump,RO}$	1120	1131	kW	0.97
M_f	485.9	485.9	m^3/h	0
SR	0.9944	0.9944	-	0
X_b	64,180	64,180	ppm	0
X_d	252	250	ppm	0.8
ΔP	6843	6850	kPa	0.1

Boiler fuel consumption is provided applying equation. (20), where $T_{setpoint}$ is the set-point temperature of the boiler, $T_{f,inlet}$ is the inlet temperature of water, f_{boiler} indicates whether the boiler is ON or OFF, and n_t is the number of time steps in modeling and problem solving. The resulting thermal comfort of the system is computed applying PMV parameter, which was assessed from the appropriate and practical criteria utilized to evaluate thermal comfort [29], which is provided by Eq. (21).

$$BFC = \frac{\sum_{i=1}^{n_t}\left(\dot{m}_f c_f \left(T_{setpoint} - T_{f,inlet}\right), f_{boiler}\right)}{h_{boiler} LHV} \tag{20}$$

$$PMV = [0.303 \times exp(-0.036M) + 0.028] \times L_B \tag{21}$$

L_b is the amount of heat load of the body of the residents of our buildings, in this regard, the parameter M represents the amount of metabolism due to the activity of people. The ASHRAE-55 standard specifies the suggested range of PMV [34] −0.5 and 0.5, and the ideal value of the PMV parameter is 0 [54].

LCC is chosen as an economic parameter to identify the economic performance of system and is presented using Eq. (22).

$$LCC = I_C + PWF \times AOC - R_I; PWF = \begin{cases} \frac{1}{d-i}\left[1 - \left(\frac{i+1}{d+1}\right)^{n_L}\right] ifi^1 d \\ \frac{n_L}{i+1} \quad ifi = d \end{cases} \tag{22}$$

I_c is the initial investment cost of the Renewable system, AOC is the amount is the operating cost of the system during one year, R_I is the resale revenue, 15% of the initial investment cost is estimated for each component [31]. PWF is the present value factor, which is computed from the inflation rate (i), discount rate (d), and system lifespan (n_L) [31].

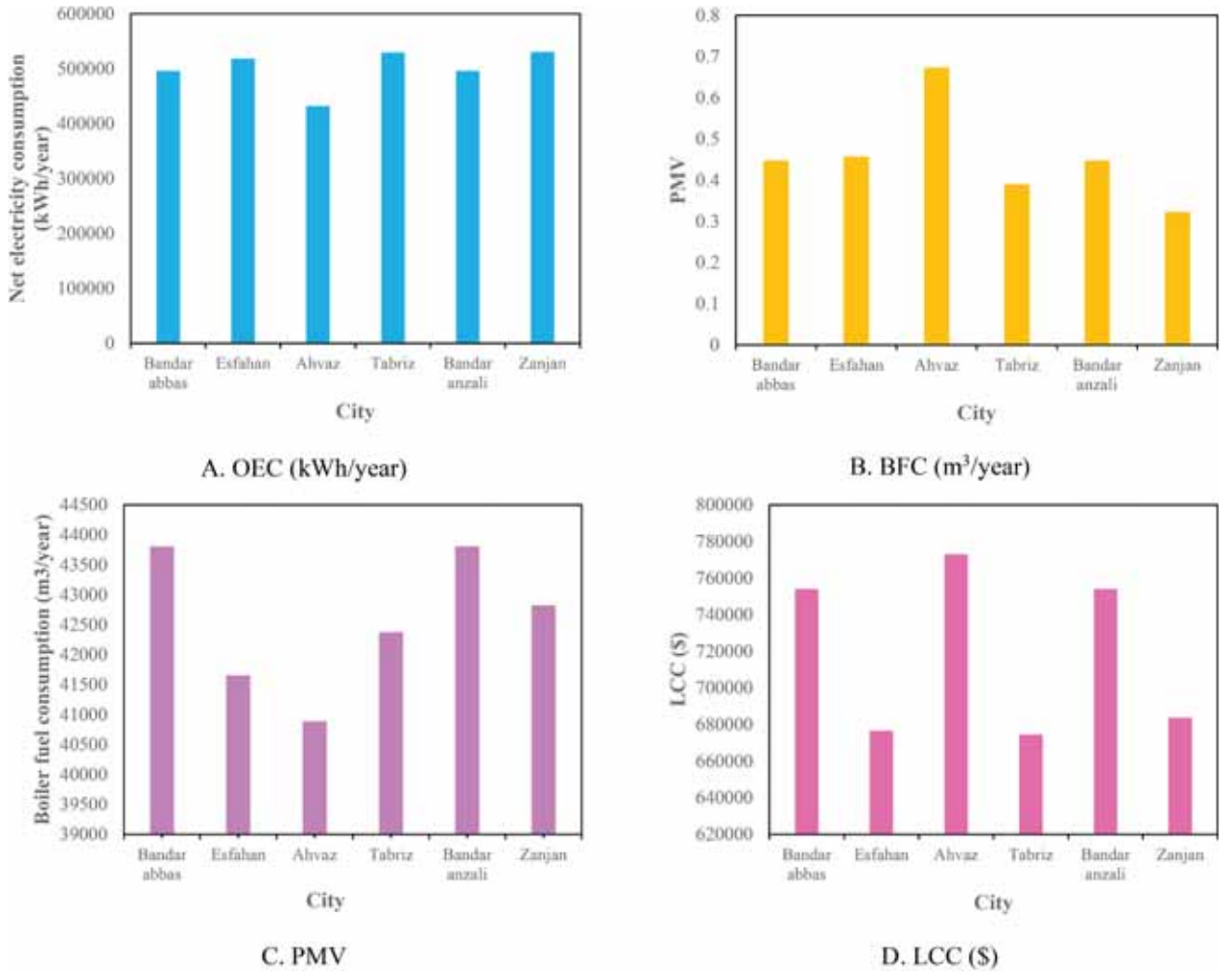

Fig. 6. Comparison of system performance in different geographical areas.

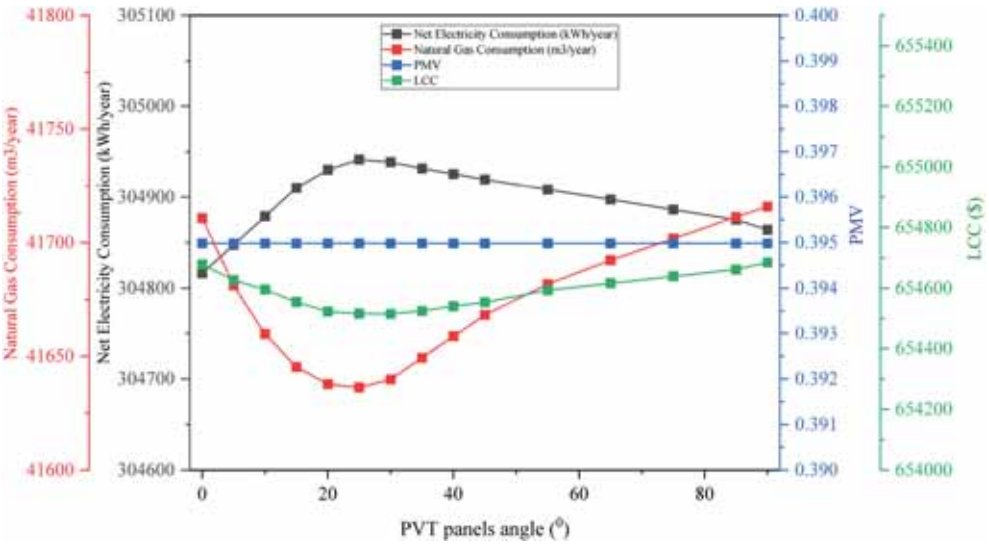

Fig. 7. Effect of PV/T panel angle on system performance.

The life cycle includes the time span from when an asset's necessity is determined to when it is decommissioned. Life cycle management is a strategy for choosing whether to buy or acquire each new asset, taking into account and managing all associated costs in various phases. Life cycle costing is a process for economic analysis and evaluation of the total costs related to purchase, installation, maintenance and repairs, refurbishment, and scrapping, and generally the total cost of ownership for equipment. We may mention cost management and reduction, choosing the best purchasing and procurement strategy, economic analysis of the plan, and economic assessment of the effectiveness of new technology as examples of the use of LCC analysis. Table 5 introduces the objective functions studied to increase the system performance and decrease the economic costs of the system and indicates the objectives of optimization method.

3. Results and discussion

3.1. Validation

Regarding the novelty of the renewable system of the present work, the reverse osmosis desalination subsystem was validated applying the study of Nafey and Sharaf [55], and Table 6 lists the results, which show high-accuracy modeling.

3.2. Comparison of cities

The impacts of weather in various places on the functioning of the system were looked into in this research in order to validate its performance. The research region includes six Iranian cities with hot, cold, and mild climates: Tabriz, Zanjan, Esfahan, Ahvaz, Bandar Anzali, and Bandar Abbas.

Tabriz has cold winters and hot, dry summers. The area's high altitude and hilly landscape have an impact on the winter cold. Ahvaz is a city with four distinct seasons, each of which has its unique charm. The finest seasons in Ahvaz, which has a very agreeable climate, are often winter and spring. Ahvaz is one of the hottest cities in Iran since there isn't much greenery there. The summer months in this city are lengthy and hot, with a rise in air temperature of up to 50°. However, the city's winters are brief and moderate, with lows of just 5°. The city of Bandar Abbas has a hot and muggy climate. Between mid-November and mid-April, the weather is often good in Bandar Abbas. May and June are dry months, but July through October are humid. On the warmest days,

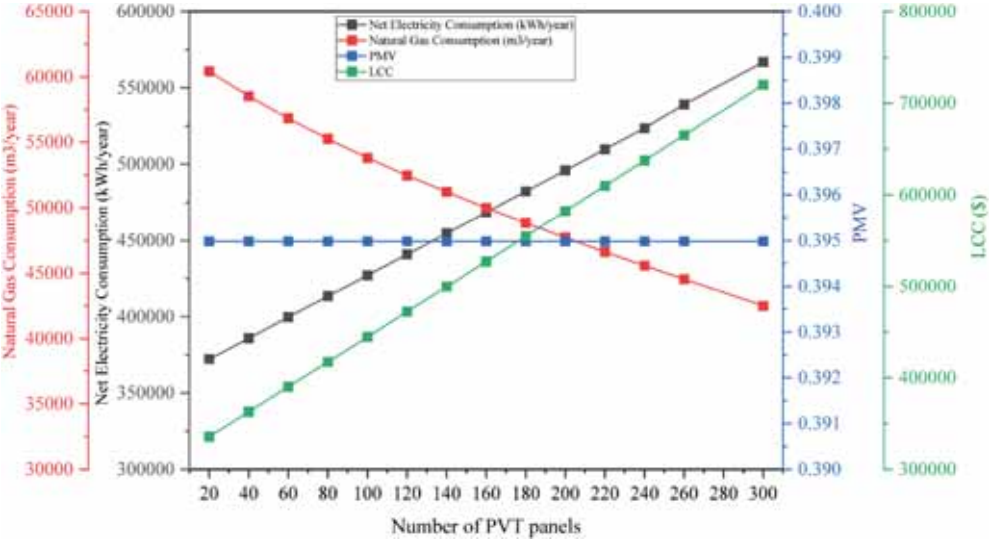

Fig. 8. Effect of number of PV/T panels on system performance.

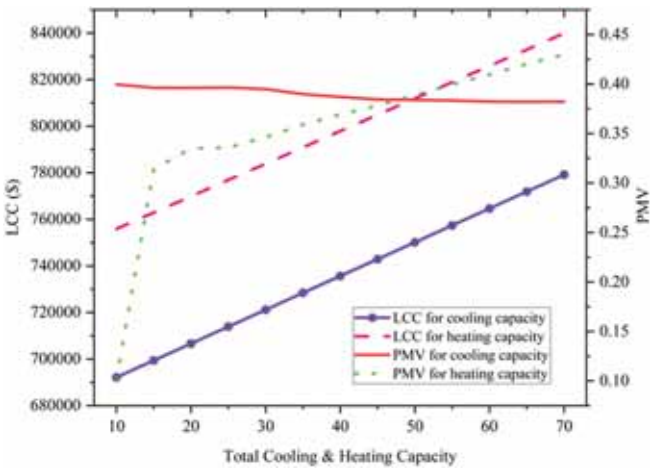

Fig. 9. The effect of HP on LCC and PMV.

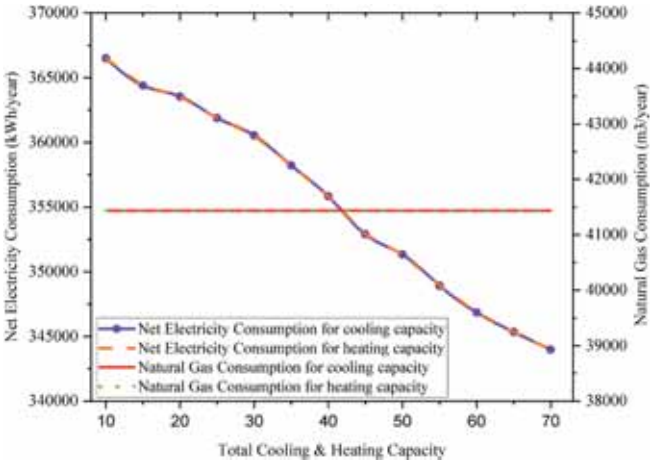

Fig. 10. The effect of HP on power and fuel consumption.

the air in Bandar Abbas city may be as hot as 52° Celsius and as cold as 2° Celsius. This city has heights with a cold mountainous climate, snowy and chilly winters, and warm and dry summers. Zanjan City has a moderate and temperate climate. In general, Bandar Anzali has hot, muggy summers and moderate, sometimes chilly winters. The climate in this seaside city is humid. The climate in Esfahan is mild and semiarid. Esfahan really has extremely hot summers because to its position in a semi-arid region. Additionally, Esfahan experiences chilly winters as a result of its location in this region.

Fig. 6 displays the analyses' findings. The findings demonstrated that Zanjan City had a higher production capacity than the other cities, and the economic analysis demonstrated that Zanjan City's implementation of this method was more cost-effective. Zanjan City was chosen for further examination because of its greater comfort level and lower boiler fuel use.

3.3. Parametric study

A parametric research has been carried out to examine the rate of growth and reduction of the four goal functions in order to assess how the system performs in response to changes in the design parameters. The impact of variations in the PVT collector angle on the goal function is seen in Fig. 7. The findings show that 26° is the ideal angle for the collection. By decreasing this angle, system expenses and fuel consumption rise while output power declines. By raising this angle, the output power declines while costs and fuel consumption rise. However, since the desired parameter is not directly connected to the generation of cooling and heating in the building, there is no influence of increasing or decreasing this parameter on the PMV.

The impact of changes in the quantity of photovoltaic panels on the goal functions is shown in Fig. 8. The findings indicated that 160 solar panels were the ideal quantity. Reducing production power increases fuel consumption while decreasing system costs. As production power grows, so do costs and fuel consumption. It is obvious that the shift in the quantity of solar panels is the cause of this. The prices and output of power grow according to the quantity of the aforementioned panels. As output rises, hot water production follows suit. The more this rise, the more the quantity of gas required to create hot water declines. The end consequence is a drop in gas consumption, as seen in the diagram. Given that the comfort factor affects the residential complex's cooling and heating and that this parameter has no bearing on the generation of cooling and heating, changes in it have no bearing on the PMV.

The impact of HP modifications on the goal functions is seen in Figs. 9 and 10. The PMV tends to drop for heating capacity and rise for cooling, which is an appropriate pattern, and Fig. 9 shows how increasing cooling and heating capacity boosts expenses. Additionally, the production power decreases proportionately to the increase in cooling and heating capabilities. Due to the fact that these two variables

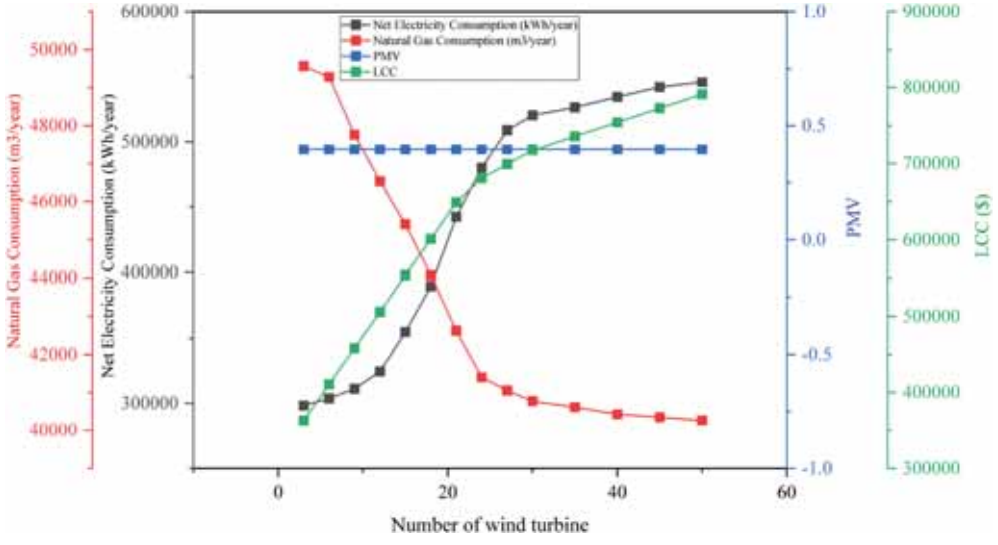

Fig. 11. The effect of the number of wind turbines on system performance.

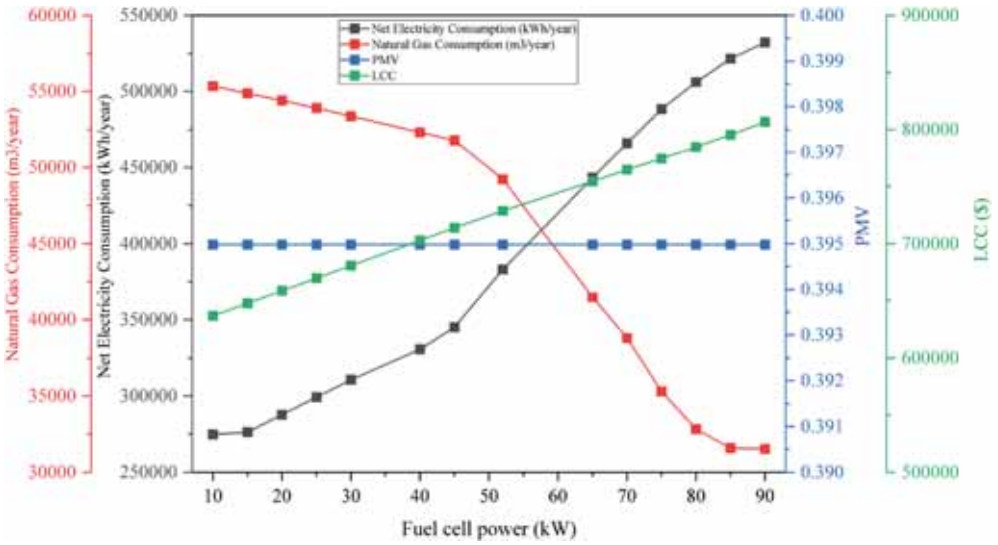

Fig. 12. Effect of fuel cell power on system performance.

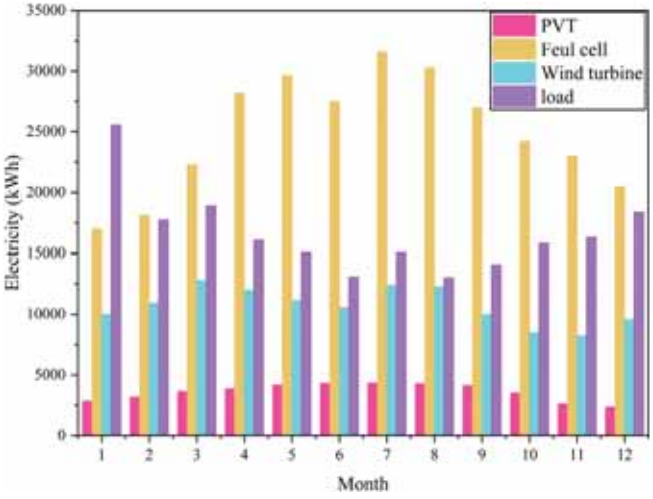

Fig. 13. Comparing the electricity produced by the units with the load.

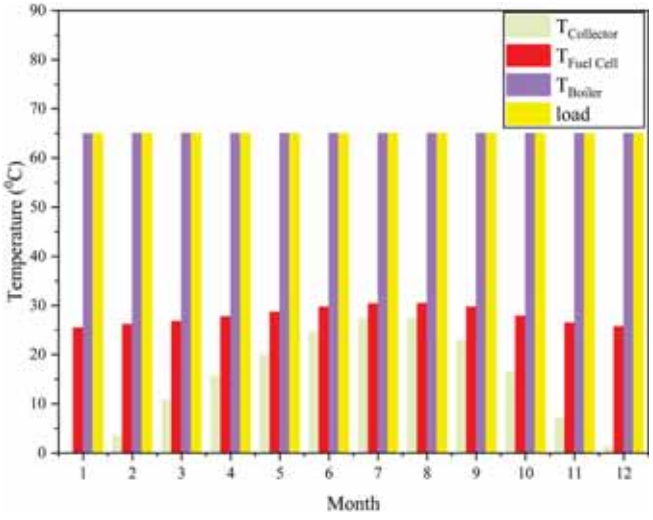

Fig. 14. Comparing the temperature of the system units with the load.

have no bearing on the system's need for producing hot water, they have no impact on fuel use.

Fig. 10 depicts the variations in the heat pump's capacity as a result of varying power production and boiler fuel consumption. According to the results of this figure, as the capacity of the heat pump increases, the amount of fuel consumed does not change, but the amount of electrical energy decreases. This is because, as the capacity of the heat pump increases, the amount of electricity required increases due to the increase in energy consumption. This decreases the quantity of power the system generates.

Additionally, as shown in Fig. 11, the impact of changes in the number of wind turbines on the goal functions was examined. The findings indicate that 20 wind turbines are the ideal amount, and by raising this number, the system's potential expenses and fuel consumption may both rise. The suggested system allocates a portion of the wind turbine's output power to the electrolyzer, which produces the fuel the fuel cell needs, which accounts for the decrease in fuel usage. The more hydrogen created as a consequence of an increase in wind turbine output, the hotter water the fuel cell will be able to produce and the less fuel will be required to do so. Reducing the quantity of the aforementioned factors will increase fuel consumption while decreasing power generation and prices. The building's capacity for cooling and heating is connected to the PMV coefficient, which is constant when these factors vary.

The impact of changes in fuel cell power on the intended performance is seen in Fig. 12. The findings demonstrate that raising the fuel cell's power increases the cost of the system in addition to the system's overall power, but it also significantly lowers fuel usage. Reducing the fuel cell's output power raises fuel consumption while also lowering system expenses and production power. This parameter does not alter the PMV since it has no impact on the generation of cooling or heating.

Fig. 13 shows the results of a study comparing the amount of power generated by the system to the amount of electricity used over the course of one year. As it turns out, solar units, fuel cell units, and wind turbine units are the generators of electricity in the renewable system of the present work. Furthermore, the results indicate that the electricity produced by the fuel cell unit throughout the year can provide all of the required energy and even produce a surplus. In addition, this figure demonstrates that the solar system can offer about one-third of the annual electrical energy demand. On the other hand, the findings indicate that the wind turbine unit may also offer a significant portion of the annual energy need. It is also feasible to split the suggested system into two sections during the day, with the first half consisting of the solar unit and wind turbine, which can fulfill the energy need, and the fuel cell unit

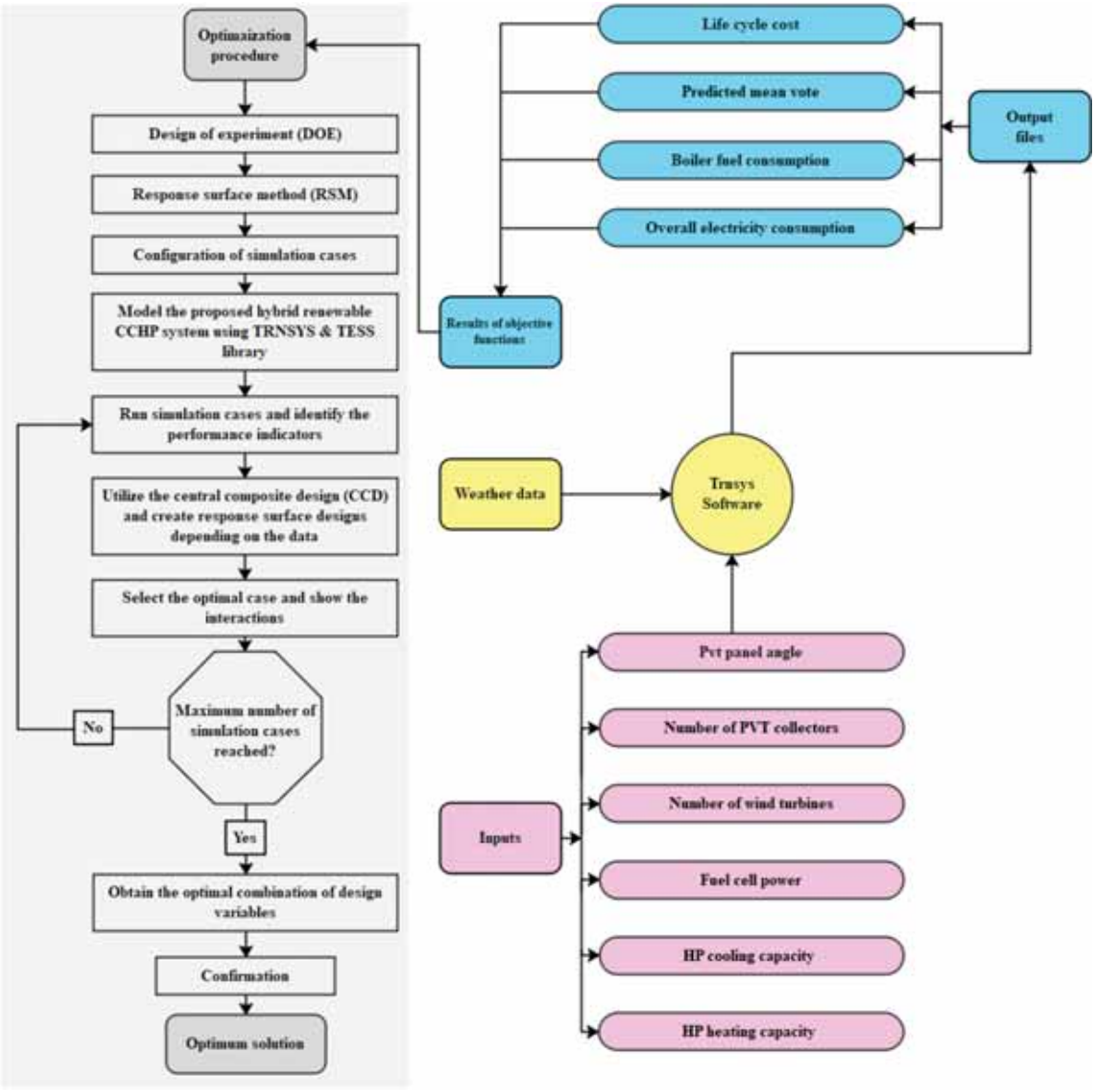

Fig. 15. The hybrid system designed in TRNSYS platform.

being utilized at night. Provide energy consumption. Because solar energy is unstable and unavailable at night and on rainy days, additional units may be employed to provide energy and operate complexes when solar energy is unavailable.

In order to examine the system's production temperature and compare it with the consumed load over the course of one year, an analysis was conducted; the findings are shown in Fig. 14. As it turns out, solar units, fuel cell units, and boilers are the heat producers in this work's renewable system. The findings indicate that the production temperature of the boiler equipment can fulfill the specified temperature rates throughout the whole year. This figure also demonstrates that the fuel cell unit can provide around fifty percent of the annual load temperature. On the other hand, the findings indicate that the collector can provide a large portion of the annual temperature need.

3.4. Optimization

Fig. 15 depicts the flowchart for the suggested approach of system optimization. In order to improve this system, six decision-making factors were analyzed, and their upper and lower limits are shown in Table 4. In addition, for a comprehensive multi-objective optimization, four objective functions impacting the system were taken into account, as shown in Table 5.

One of the tools for designing experiments is the Response Surface Methodology, which is a collection of mathematical techniques that establish the link between one or more response variables and a number of independent factors. Optimizing the response (output variable), which is influenced by a number of independent factors, is the aim of response surface designs (input variables). Execution tests are the tests that make up an experiment. To identify the reasons for changes in the response variable, the input variables are altered in each experiment. Building response procedure models is an iterative process in response-level designs. Once a rough model has been created, it is assessed using the goodness of fit approach to see if the result is adequate or not. More tests are run and the estimating procedure begins again if the solution is not verified. The objective of experiment design is to determine and examine the factors influencing the outcomes using the fewest possible experiments. The steps in the response level approach are as follows:

Tests to screen for efficient input variables.

- Regression analysis to estimate the fitting function of outputs due to inputs.
- Optimization in order to identify the optimal levels of input variables.

Table 7
The simulation results.

	Factors						Responses			
Run	Photovoltaic panel angle	Number of PVT panels	Number of wind turbine	Fuel cell power	Heat pump cooling capacity	Heat pump heating capacity	Net electricity consumption kWh/year	Boiler fuel consumption	PMV	LCC
1	73.7524	72.2114	5.41585	65.5577	49.1683	49.1683	−116355	58967.6	0.376135	893037
2	73.7524	327.789	24.5841	14.4423	49.1683	10.8317	−2800.15	55877.1	0.150117	498582
3	45	200	0	40	30	30	92547.6	48009.3	0.693388	949018
4	26.2476	327.789	24.5841	14.4423	49.1683	49.1683	18337.7	54268	0.752183	897267
5	26.2476	72.2114	24.5841	14.4423	49.1683	10.8317	−102819	59121.6	0.3002	489586
6	73.7524	327.789	24.5841	14.4423	10.8317	49.1683	744.24	55888.4	0.774255	842117
7	45	0	15	40	30	30	−4774.27	62480.3	0.693388	598845
8	45	400	15	40	30	30	178242	42187.5	0.693388	544170
9	26.2476	72.2114	5.41585	65.5577	49.1683	10.8317	56867.5	55808.7	0.181668	546087
10	26.2476	327.789	5.41585	65.5577	49.1683	49.1683	182269	40209.1	0.751427	447320
11	73.7524	327.789	24.5841	65.5577	49.1683	49.1683	370665	36753.3	0.751427	688705
12	26.2476	72.2114	24.5841	65.5577	10.8317	10.8317	288020	54720.9	0.317503	807063
13	26.2476	327.789	24.5841	65.5577	10.8317	49.1683	393153	35829.7	0.772602	17429.7
14	26.2476	72.2114	24.5841	65.5577	49.1683	49.1683	284115	54720	0.751427	42469.7
15	45	200	15	40	30	30	18229.8	53043	0.693388	369816
16	26.2476	327.789	5.41585	14.4423	10.8317	49.1683	−79695.6	54814.8	0.77262	987631
17	73.7524	72.2114	24.5841	14.4423	49.1683	49.1683	−120700	60197.1	0.751427	934511
18	26.2476	72.2114	5.41585	14.4423	49.1683	49.1683	−209097	59257.6	0.751427	971793
19	45	200	15	40	30	60	18236.8	53043	0.822625	929790
20	26.2476	327.789	5.41585	14.4423	49.1683	10.8317	−9185.5	54803.4	0.181668	971790
21	45	200	15	80	30	30	385015	41896.2	0.693388	971790
22	73.7524	72.2114	5.41585	65.5577	10.8317	10.8317	−113151	58972.1	0.34288	971790
23	26.2476	327.789	5.41585	65.5577	10.8317	10.8317	17910	49667.2	0.34288	971790
24	45	200	15	40	60	30	14161	53035.9	0.666138	971790
25	45	200	15	40	30	30	17946.2	53035.9	0.693388	971790
26	45	200	15	40	30	30	17946.2	53035.9	0.693388	971790
27	73.7524	72.2114	24.5841	65.5577	10.8317	49.1683	194127	56869.6	0.77262	900554
28	73.7524	72.2114	5.41585	14.4423	49.1683	10.8317	−218293	60197.1	0.181668	987654
29	73.7524	327.789	24.5841	65.5577	10.8317	10.8317	285597	42302.7	0.203339	988754
30	73.7524	72.2114	5.41585	14.4423	10.8317	49.1683	−214330	60197.1	0.77262	972088
31	73.7524	72.2114	24.5841	65.5577	49.1683	10.8317	190163	56869.6	0.181668	991235
32	73.7524	327.789	5.41585	65.5577	49.1683	10.8317	−7303.74	51244	0.181668	997876
33	45	200	30	40	30	30	96149.3	53027.6	0.693388	954896
34	26.2476	327.789	24.5841	65.5577	49.1683	10.8317	299649	41273.2	0.181668	695804
35	45	200	15	40	30	30	17946.2	53035.9	0.693388	956813
36	45	200	15	40	0	30	21560.3	53035.9	0.744255	843316
37	26.2476	72.2114	24.5841	14.4423	10.8317	49.1683	−108471	59257.6	0.77262	973164
38	45	200	15	40	30	30	17946.2	53035.9	0.693388	841404
39	0	200	15	40	30	30	5556.09	53735.5	0.693388	990509
40	45	200	15	40	30	20	17967	53035.9	0.698764	599974
41	26.2476	327.789	24.5841	14.4423	10.8317	10.8317	14361.3	54662.3	0.203339	788355
42	73.7524	72.2114	24.5841	14.4423	10.8317	10.8317	−116672	60197.1	0.203339	988650
43	90	200	15	40	30	30	−20043.2	56267.4	0.693388	897614
44	45	200	15	40	30	30	17946.2	53035.9	0.693388	916498
45	73.7524	327.789	5.41585	14.4423	10.8317	10.8317	−105198	56279.6	0.203339	546700
46	45	200	15	40	30	30	17946.2	53035.9	0.693388	655958
47	45	200	15	40	30	30	17946.2	53035.9	0.693388	935378
48	45	200	15	0	30	30	−111668	134701	0.693388	987865
49	73.7524	327.789	5.41585	65.5577	10.8317	49.1683	−3339.83	51244	0.77262	431810
50	73.7524	327.789	5.41585	14.4423	49.1683	49.1683	−109225	56279.6	0.751427	541071
51	26.2476	72.2114	5.41585	65.5577	10.8317	49.1683	−104654	58035.7	0.77262	485883
52	26.2476	72.2114	5.41585	14.4423	10.8317	10.8317	−205069	59252.7	0.203339	487799

3.4.1. Optimization results

Experiment design is one of the most essential subjects covered in a variety of sectors, particularly laboratory operations. In actuality, statistical design for experimental studies is regarded as a fundamental concept in laboratory and industry research. These designs provide more trustworthy findings, save time, decrease the number of tests dramatically, and eventually lead to process improvement. Before an experiment is conducted, the design of the experiment is a valuable way for analyzing data to arrive at reliable and objective results. It is feasible to establish the ideal value of measurement findings (answers) or the circumstances under which contradictory responses are compatible by using experimental designs.

The initial stage in optimization using the RSM technique and Design Expert software is to input the number of design variables and their

Table 8
Optimal results for decision variables.

description	The angle of photovoltaic panels (°)	Number of photovoltaic panels (−)	Number of wind turbines (−)	Fuel cell power (kW)	Heat pumpcooling capacity (kW)	Heat pumpheating capacity (kW)
Optimal design	*26*	*106*	*2*	*65.6*	*48.7*	*20.2*

Table 9
Comparison of optimization results with modeling results.

Objective function	OEC (kWh/year)	BFC (m^3/year)	PMV	LCC ($)
Result of RSM	*−237859.7418*	*42310.17293*	*0.429*	*689651.9*
Confirmation	*−225694.7925*	*41435.87595*	*0.413*	*674278.4*
Prediction error (%)	*5.39*	*2.11*	*4.29*	*2.28*

ranges. Following this, 52 iterations were deemed necessary to do a comprehensive optimization, and finally, the optimal design was determined. By calculating the value of the objective functions in each step using the Trnsys software and inputting the ideal value for each iteration, the Expert Design software will ultimately provide 100 optimal options, the best of which will be the solution for the first stage. The results of computing the number of 52 optimization runs are shown in Table 7.

One hundred optimum solutions for decision variables and objective functions are generated after inputting the output results from Trnsys software into Design Expert software; the best solution is the answer to the first step. The optimal outcome for the decision variables is shown in Table 8, and the results indicate that the optimal values for the photovoltaic panel angle, number of panels, wind turbine, fuel cell power, cooling capacity, and heating capacity are 26°, 106 photovoltaic panels, 24 wind turbines, 65.6 kW of fuel cell power, and 20.2 kW of heating capacity.

Table 9 displays the suggested system's optimum performance outcomes. This table shows the RSM method's optimization findings together with the outcomes of a system performance simulation conducted prior to optimization. The greatest amount of inaccuracy in the optimization approach is 5.39%, according to analysis of the system's performance in two modes of simulation and optimization and comparison of the findings. Additionally, it was determined that the objective functions of total annual power consumption, boiler fuel consumption, comfort factor, and life cycle cost were, respectively, −225694.7925 kW h, 41435.87595 cubic meters, 0.413%, and 674278.4 dollars. Total power consumption with a negative sign indicates that more energy is produced than is used by the system, and this extra energy is sold to the grid.

3.4.2. Interactions of design variables

This section discusses the effects of decision-making variables on the system's goal functions in order to enhance its performance. The performance of the system is shown in Fig. 16a as a function of the fuel cell's power and the solar panel's angle. As can be seen, raising these two values leads to an increase in net power usage. Increasing the solar panel's efficiency increases the generation of renewable energy, which in turn increases power. Fig. 16b demonstrates that the number of wind turbines and solar panels has a large impact on the OEC and greatly raises net electricity consumption. The impact of heat pump cooling and

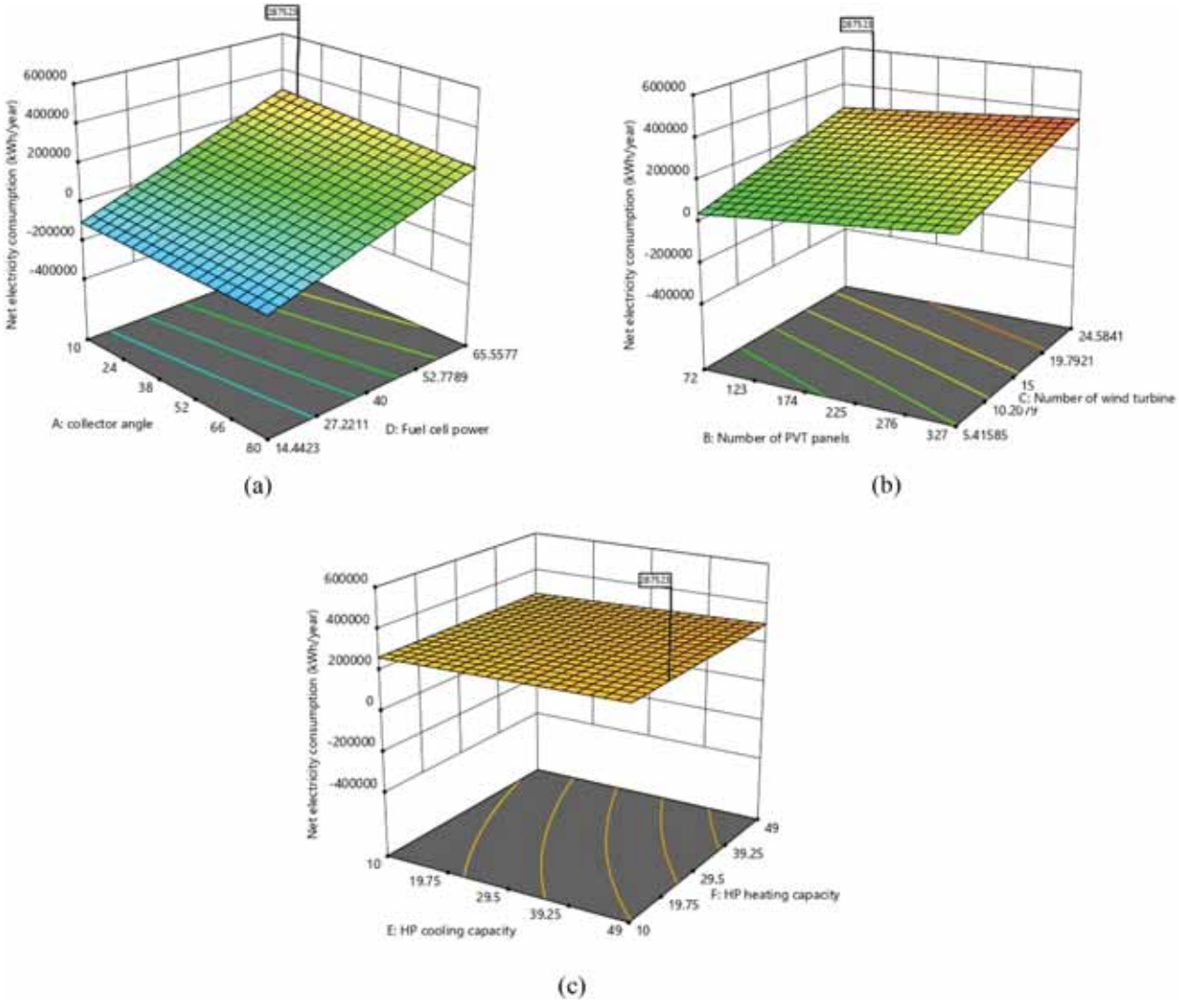

Fig. 16. The effect of changes in decision making variables on the overall electricity consumption.

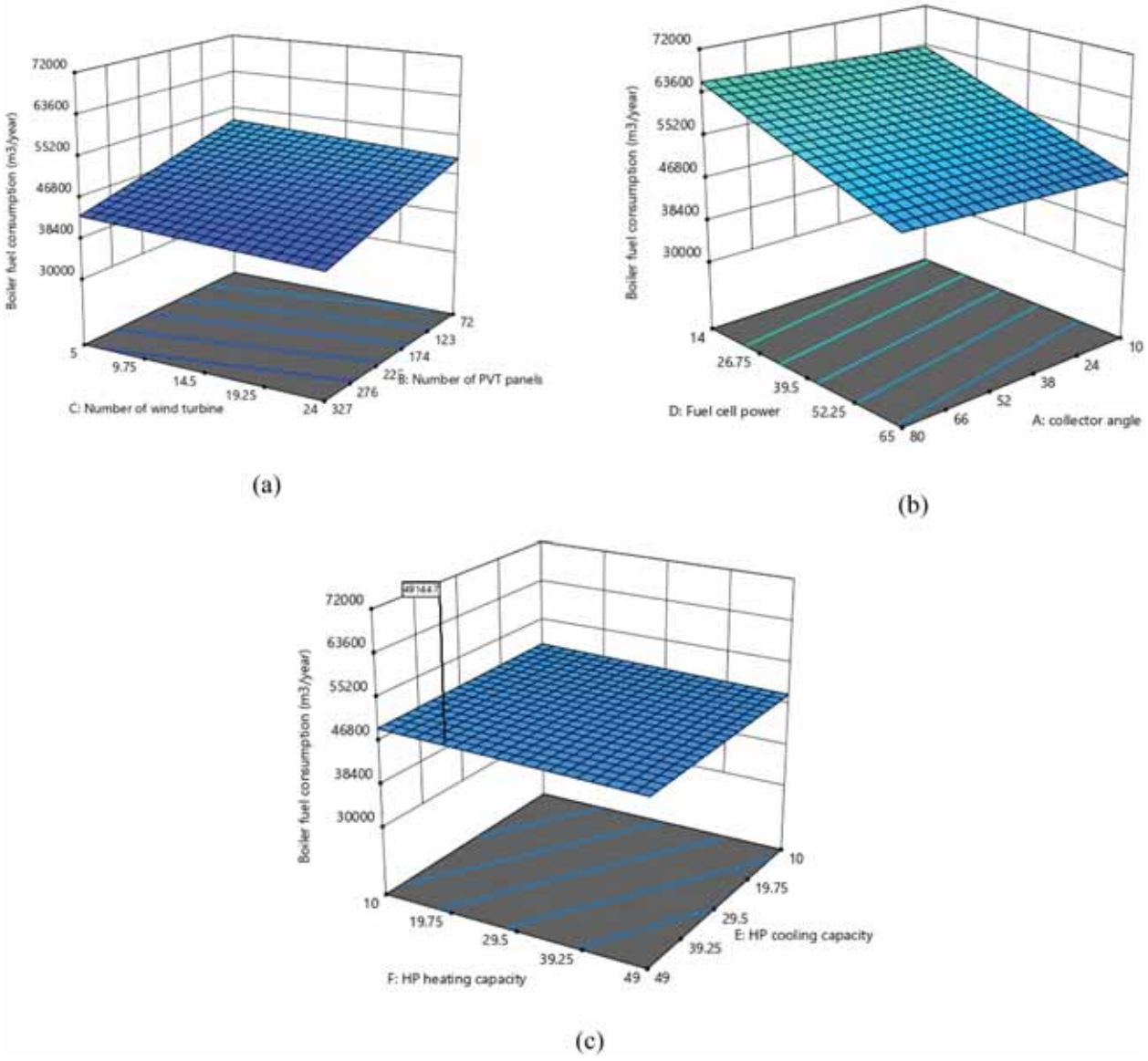

Fig. 17. The effect of changes in decision making variables on the boiler fuel consumption.

heating capacity on net power consumption is shown in Fig. 16c. Low power output is the outcome of the heat pump's large cooling and heating capacity since these heat pumps require more electricity than those with smaller cooling and heating capabilities. Until the thermal comfort response (PMV) stays ideal, the optimization procedure seeks to choose reduced values for the heat pump's heating and cooling capacity.

The impact of the quantity of solar panels and wind turbines on the fuel consumption of the backup boiler is shown in Fig. 17a. The backup boiler's fuel consumption is influenced by the quantity of solar panels; however, the backup boiler's fuel consumption is unaffected by the number of wind turbines. The fuel consumption of the backup boiler was reduced annually by increasing the number of thermal and photovoltaic panels. Because there are more photovoltaic/thermal panels, there is also more thermal energy available for hot water usage. In the end, this results in a decrease in the backup boiler's performance and fuel usage. Additionally, Fig. 17b demonstrates how boosting the fuel cell's output enhances the backup boiler's fuel efficiency. However, altering the collector angle and straying from the ideal angle causes the backup boiler's fuel consumption to rise. The mutual impact of heat pump cooling and heating capacity on backup boiler fuel consumption is shown in Fig. 17c. These two variables don't directly affect how much hot water is produced, thus they don't affect how much fuel the backup boiler uses.

This paper analyzed the thermal comfort supplied by the renewable system using the PMV parameter, which shows the thermal comfort value of the building. The closer the PMV is near a negative figure, the colder the building and the individual feel. The optimal value for PMV, which is presented as the ideal value, is zero, and values near to zero are associated with improved building conditions and thermal comfort for occupants. Fig. 18a, b, and c illustrate the reciprocal impacts of certain parameters on PMV. According to the data, the number of photovoltaic/thermal panels, their angle, the number of wind turbines, and the fuel cell power had no influence on PMV. In contrast, PMV was affected by heat pump cooling and heating capacity and other design elements influencing thermal comfort.

As seen in Fig. 18b, as the heat pump's cooling capacity grew from 0 to around 50 kW, PMV neared 0. It reduced from around 1 to 0.2 and rose further as the heat pump's cooling capability grew. Fig. 18c demonstrates that when the heat pump's heating capacity increases, the PMV deviates more from zero. However, an increase in the heat pump's heating capacity shifts the PMV farther away from the optimum value of zero and toward positive values. Higher values for the heating capacity

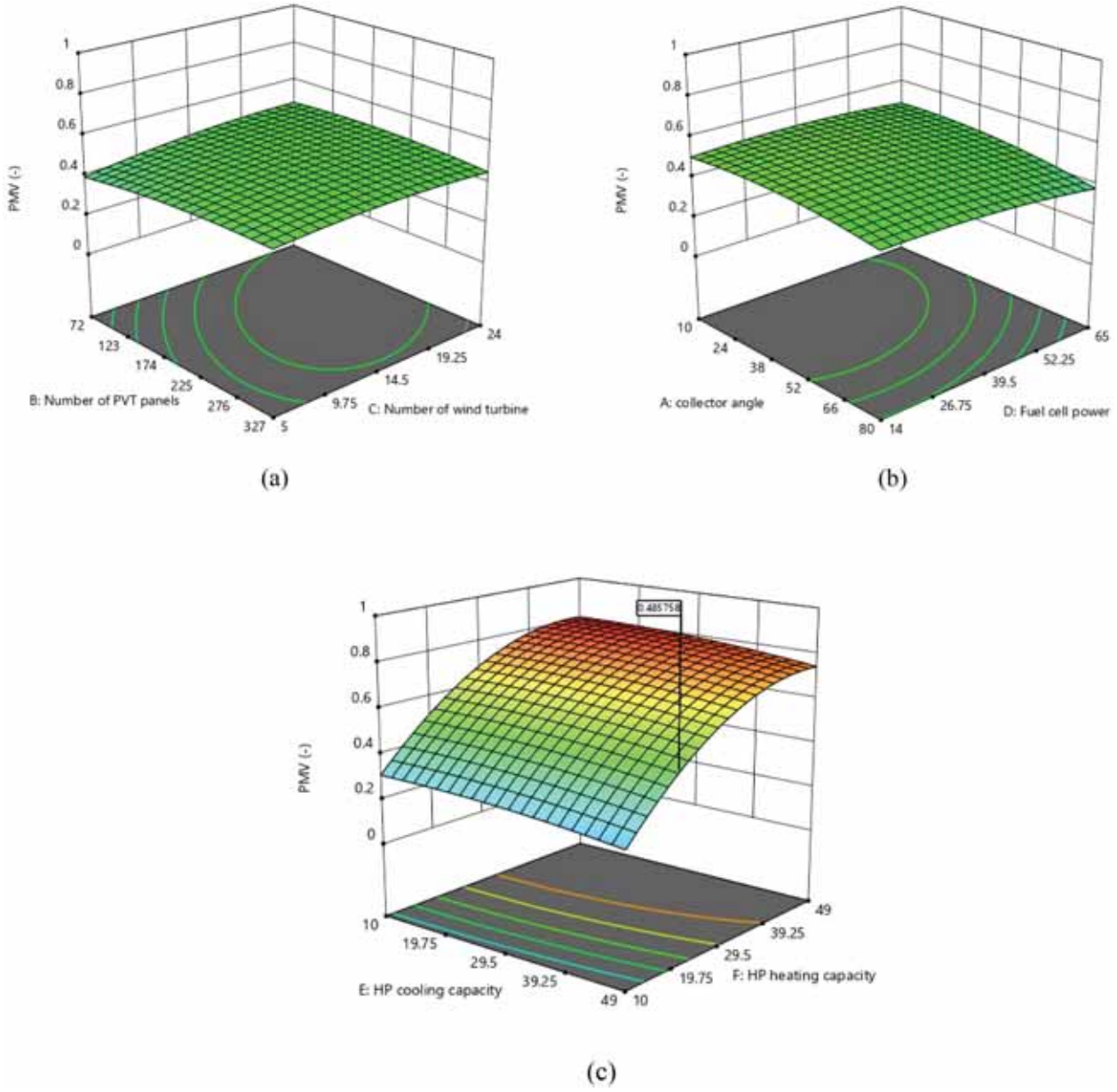

Fig. 18. The effect of changes in decision making variables on PMV.

of the heat pump lead to an increase in the thermal comfort index of PMV as the interior air temperature rises.

The cost of the suggested cycle's equipment life cycle is shown in Fig. 19a along with the interactions between the quantity of solar panels and wind turbines. The life cycle cost of the equipment grew as more solar and wind turbines were installed. Fig. 19b demonstrates how a device's life cycle cost rises as its heating and cooling capacity increases. The life cycle cost of the equipment rose when the collector angle and fuel cell power increased, as illustrated in Fig. 19c. This increase is due to the fact that a heat pump with a larger capacity costs more up front and uses more power overall.

In Fig. 20, the single-objective Pareto diagram indicates the optimal findings of the objective functions and the load distribution indicates the changes in the objective functions.

Finally, in Table 10, the complete optimized results of objective functions and decision variables are presented.

3.5. Dynamic performance of system

In this section, the system's performance and the output power of units and equipment such as wind turbines, solar panels, and fuel cells are evaluated. In Fig. 21a, the total electricity required by the designed building (red diagram) and the amount of electricity produced by the system (blue diagram) as well as the amount of electrical energy purchased from the national electricity distribution network (pink diagram) over the course of one year are analyzed and calculated hourly (8760 h). In the first two months of the year, the amount of electricity needed exceeds the amount of electricity produced by the system, necessitating the purchase of electricity. However, in the remaining months of the year, the investigated system can supply the building's electricity needs and even exceed them. The system's surplus power may be sold to the national electricity distribution network to fund system maintenance expenses. In Fig. 21b, the production power of the three fuel cell, photovoltaic, and wind turbine production units has been divided into three independent amounts for the purpose of clarity.

The 100-unit building is divided into four sections, each section

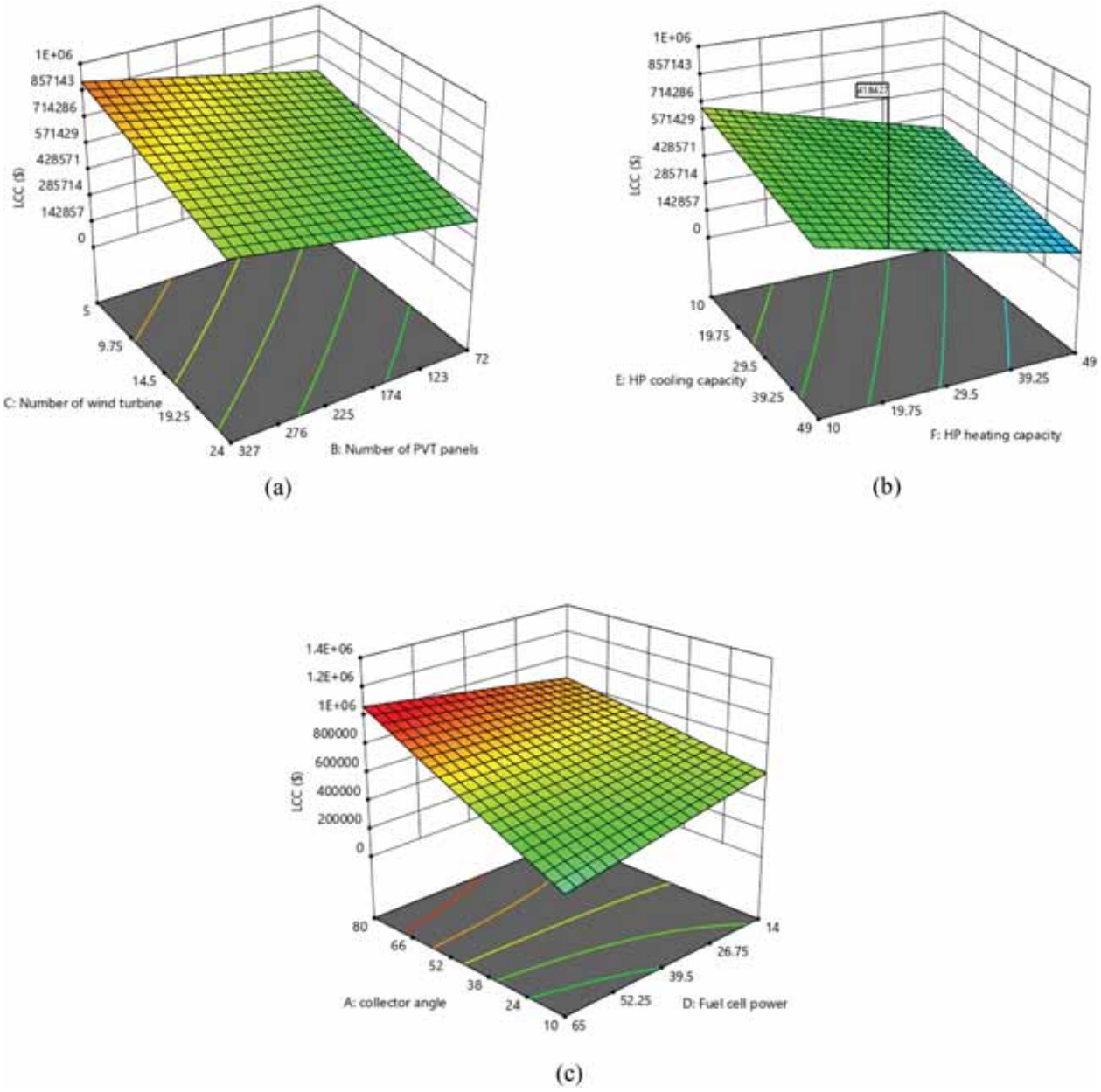

Fig. 19. The effect of interactions of design variables on the life cycle cost: effects of changing factors (a) A and B, (b) C and D, and (c) D and E.

representing a distinct zone, and each zone has a particular cooling and heating load. In Fig. 22, the needed temperatures for all four zones are estimated hourly as well as variations in ambient temperature over the course of the year (8760 9 h throughout the year). As the data demonstrate, as the ambient temperature rises during the summer and in the months of June and July, the need for cooling load rises owing to the heat of the air, and as the ambient temperature drops during the winter months, the demand for heating load grows due to In order for the building's coefficient of thermal comfort to achieve a balanced level, the building grows, and it should be noted that the consumption of cooling energy is tied to the summer months and the consumption of heating energy is related to the winter months. The findings revealed that the air temperature varies between 20 °C and a high of 26 °C, demonstrating that the present solar-wind renewable system operates well throughout the year.

Fig. 23 depicts the hourly changes in the output temperatures from the solar panel, the fuel cell, the boiler intake temperature, and the boiler outlet temperature throughout the course of the year (8760 h). Additionally, for the sake of clarity, the temperature of each unit has been split and put individually in this Fig. The findings indicate that the output temperature from the photovoltaic panel is lower in the winter, autumn, and spring months than in the summer because of a drop in solar radiation and a rise in ambient temperature. Because the photovoltaic panel cannot raise the water's temperature as much in the winter as it can in the summer, the thermal energy for the system is provided by the backup boiler and fuel cell, which can raise the temperature to about 35–40° Celsius. As a result, the fuel cell's temperature rises in the summer, in contrast to the photovoltaic panel. The boiler then raises the incoming water's temperature to 65° Celsius before transporting it to the building in issue as domestic hot water. The output temperature of a photovoltaic panel in the hot seasons is greater than the output temperature in the cold seasons because the intensity of solar radiation is higher in the summer than in the winter. Additionally, the fuel cell unit raises the water's temperature to a maximum of 75 °C, which even with the rise surpasses the boiler's set point temperature of 65 °C. In light of this, it should be noted that boiler fuel consumption is much lower in the

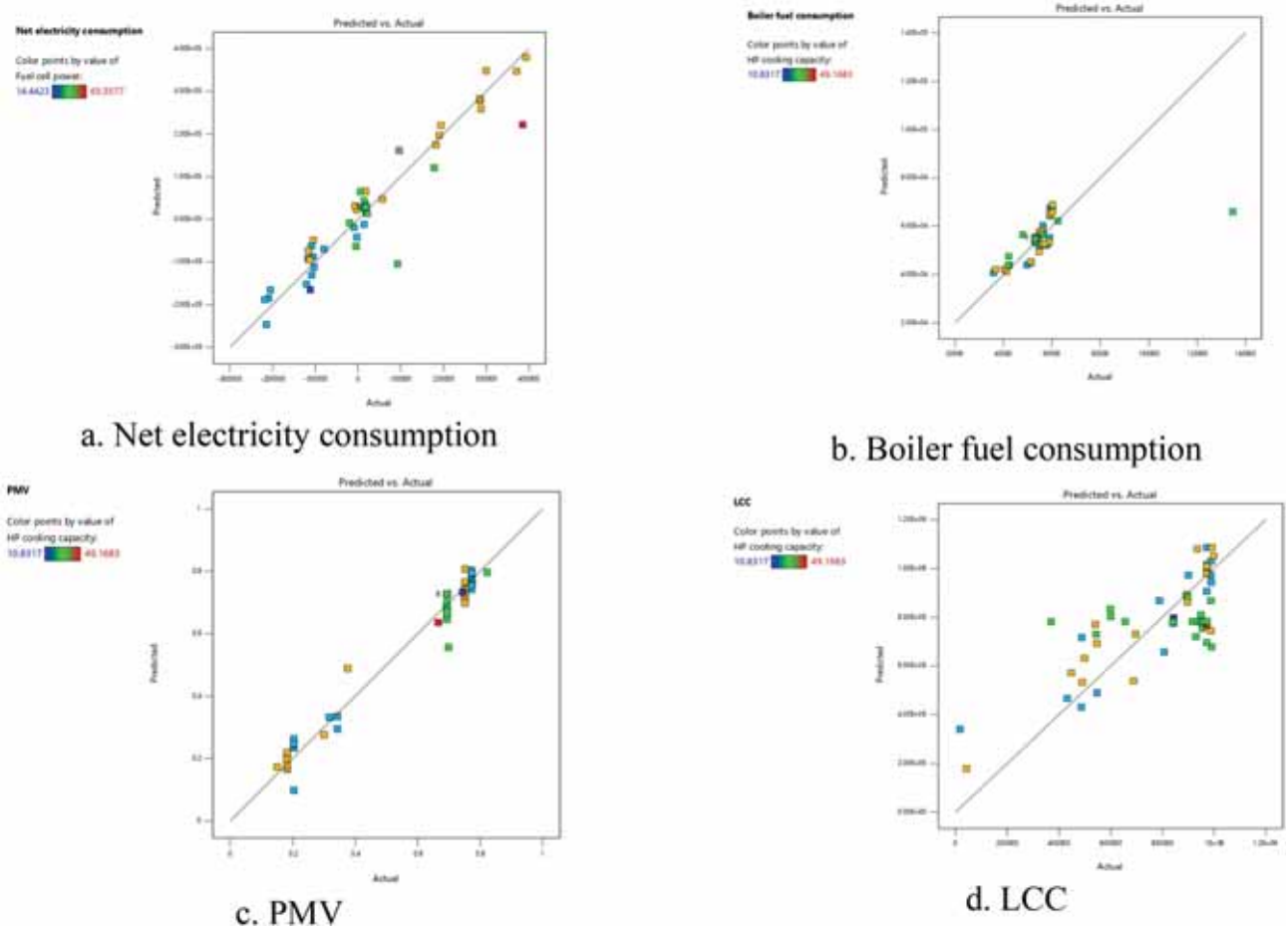

Fig. 20. Single-objective optimal results of the functions.

Table 10
Optimal results.

Row	Parameter	Value
1	*The angle of photovoltaic panels (°)*	*26*
2	*Number of photovoltaic panels (−)*	*106*
3	*Number of wind turbines (−)*	*2*
4	*Fuel cell power (kW)*	*65.6*
5	*Heat pump cooling capacity (kW)*	*48.7*
6	*Heat pump heating capacity (kW)*	*20.2*
7	*OEC (kWh/year)*	*−237859.7418*
8	*BFC (m^3/year)*	*42310.17293*
9	*PMV (−)*	*0.429*
10	*LCC ($)*	*689651.9*

summer than it is in the winter.

The battery unit and the hydrogen storage unit, two energy storage units employed in the proposed system, are shown in Fig. 24 together with their yearly hourly variations in energy storage. From December to May, the battery storage system is under strain. The amount of hydrogen in the storage tank is decreased because the battery unit and hydrogen storage tank operate in the opposite directions. Battery charge ranges from 80 to 100%. rest. Because they can sustain the level of energy storage, the findings demonstrate that employing a battery storage unit and a hydrogen storage tank simultaneously as two energy storage systems may effectively minimize the uncertainty of supply and demand differences.

The findings for the annual production of fresh water are shown in Fig. 25. The findings indicate that reverse osmosis obtains more electrical energy throughout the summer and the months of June and July as a consequence of the system's increased production capacity and decreased power use. As a result, the system produces more fresh water. The quantity of fresh water generated during this process falls when energy consumption rises owing to a reduction in energy input to the reverse osmosis desalination unit, and it is at its lowest during the spring and autumn months. The reverse osmosis process is reverse osmosis. Osmosis occurs naturally without the need of energy, but to reverse the process, energy must be added to a highly salinized solution. Water molecules may travel through a semi-permeable membrane called a reverse osmosis membrane. For the movement of bacteria, chemical compounds, and soluble salts, this option does not exist. However, you have to exert pressure to force water through the semipermeable barrier. In the process of desalination (ionization), this pressure is inherently greater than the osmotic pressure. Reverse osmosis uses a high-pressure pump to increase the pressure on the side of the salt solution. The pump runs on electricity, and the energy generated by the proposed system provides the power needed by the pump. The semi-permeable membrane is forced to let the water through by this pressure. The water removes all the dissolved salts in this manner. The feed water's concentration affects the necessary pressure. More pressure is needed to overcome the osmotic pressure the greater the input water concentration.

4. Conclusions

Given that fossil fuel supplies are depleting and there is environmental degradation from excessive carbon dioxide emissions, it is important to focus on renewable energies to meet the energy needs of residential structures. Due to the two sources of solar and wind energy

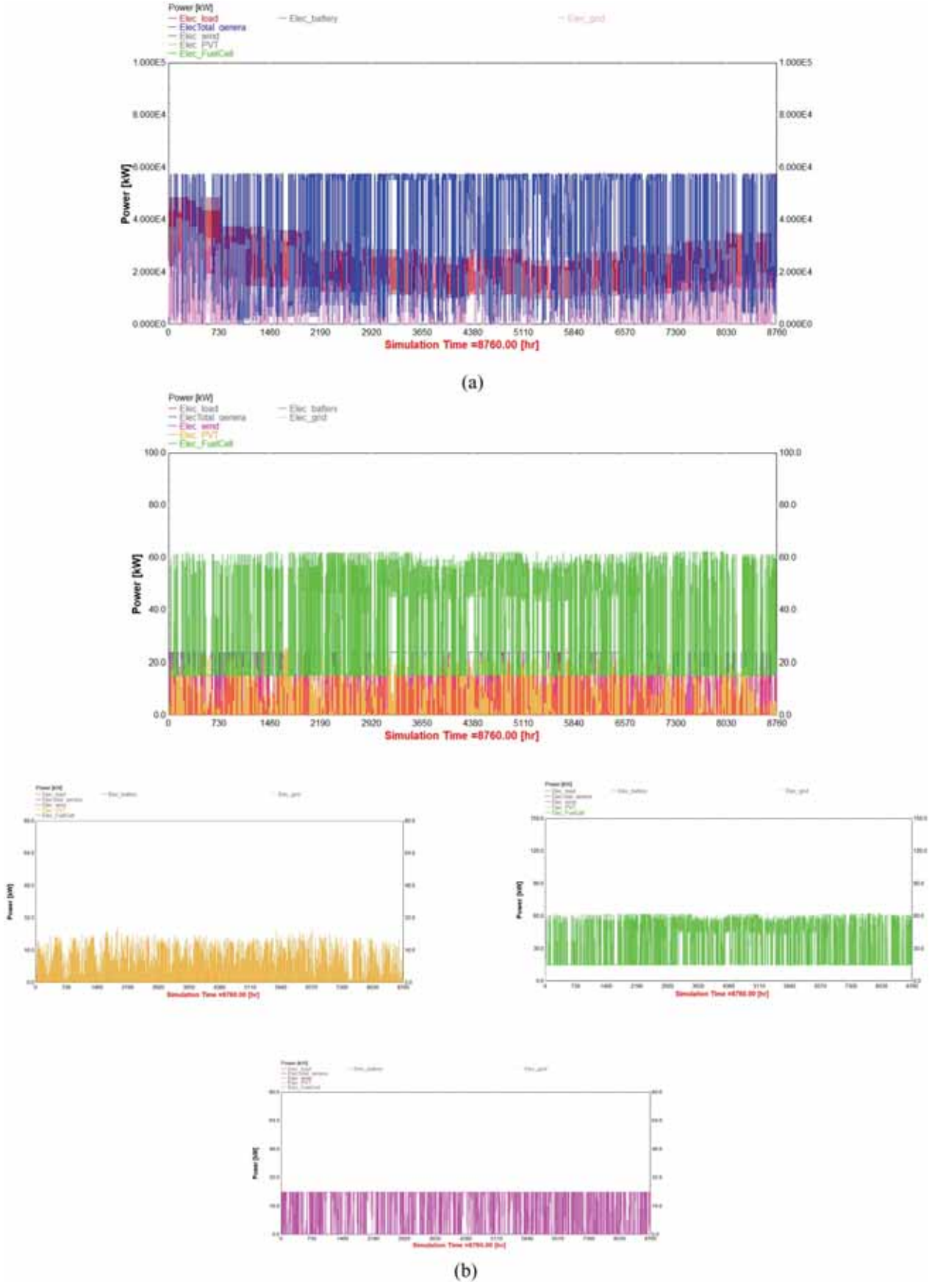

Fig. 21. Comparing the amount of electricity produced by the entire system and the amount of electricity consumed (b) Checking the amount of power produced by the system units.

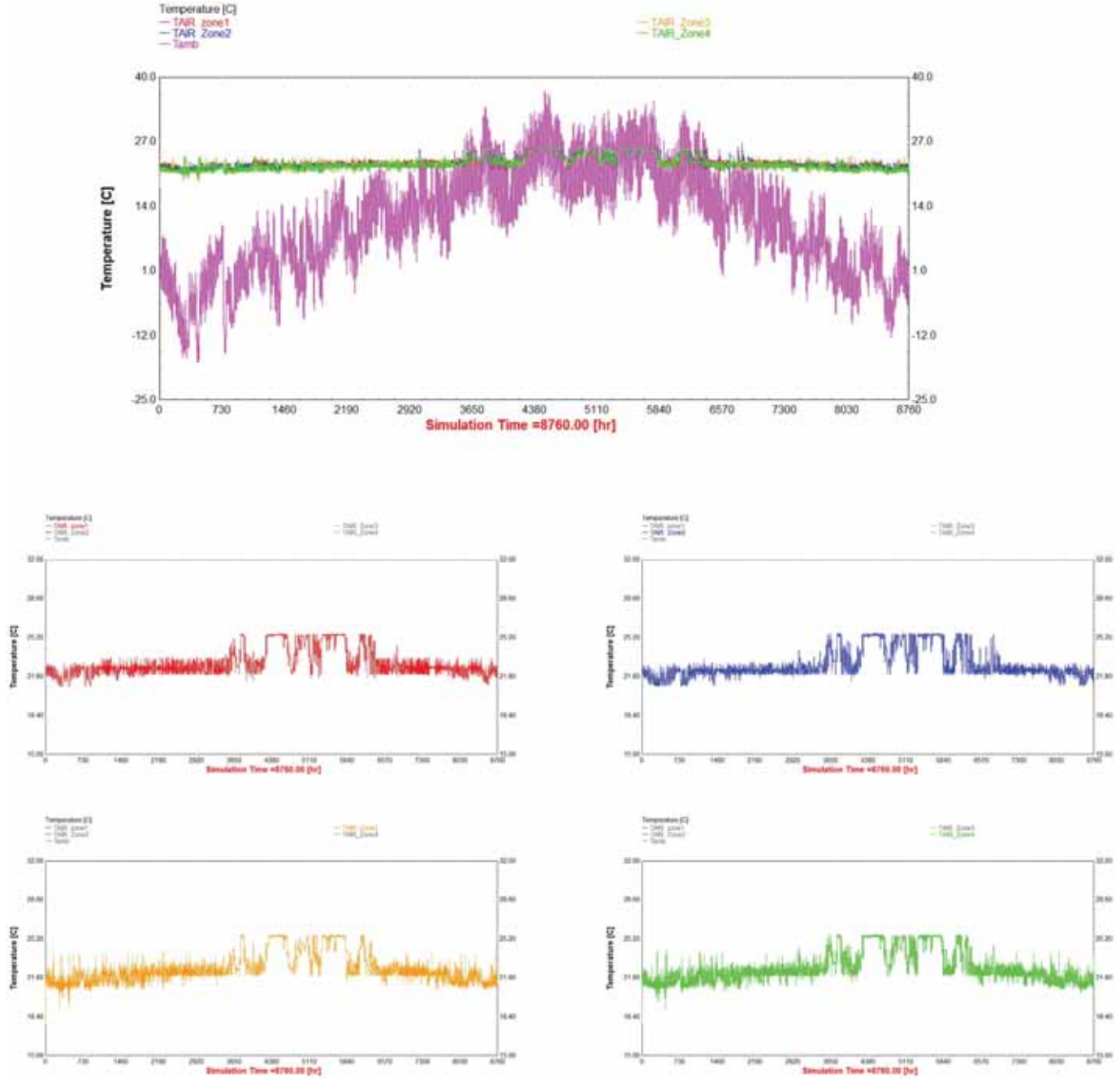

Fig. 22. Ambient temperature changes and 4 selected areas.

being potent sources, consideration has been given to addressing the demands of residential units in the present study. Using solar and wind energy in conjunction with rechargeable batteries, hydrogen production, and 100 residential units, a system was presented in this research to provide heating, cooling, hot water, fresh water, and power. An investigation of the subsystem's technical and economic aspects was done. A parametric research and sensitivity analysis of the system's design parameters, multi-objective system optimization, and a case study for the cities of Iran have all been carried out to evaluate the system's performance, and the best city to launch the suggested system has been identified.

Rechargeable batteries, fuel cells, heat pumps, photovoltaic/thermal collectors, wind turbines, hydrogen storage tanks, electrolyzers, and reverse osmosis are all components of the study's multiple production system. The main controller's design parameters, including the primary controller's angle, number, and fuel cell capacity, as well as the quantity of production heating and cooling provided by heat pump equipment, were optimized using RSM and transient modeling in TRNSYS. In addition, the effectiveness of the given design parameters was assessed using important system performance measurements. It was discovered what the main factors were for system energy consumption, boiler auxiliary fuel usage, and overall power consumption. The system's thermal comfort score was chosen as the PMV, while the LCC served as the analysis's economic criteria.

The summary of the results of this study can be stated as follows.

- The city of Zanjan was chosen as the case study, and the climate changes in this city, such as the intensity of solar radiation, ambient temperature, and wind speed, were annually analyzed.

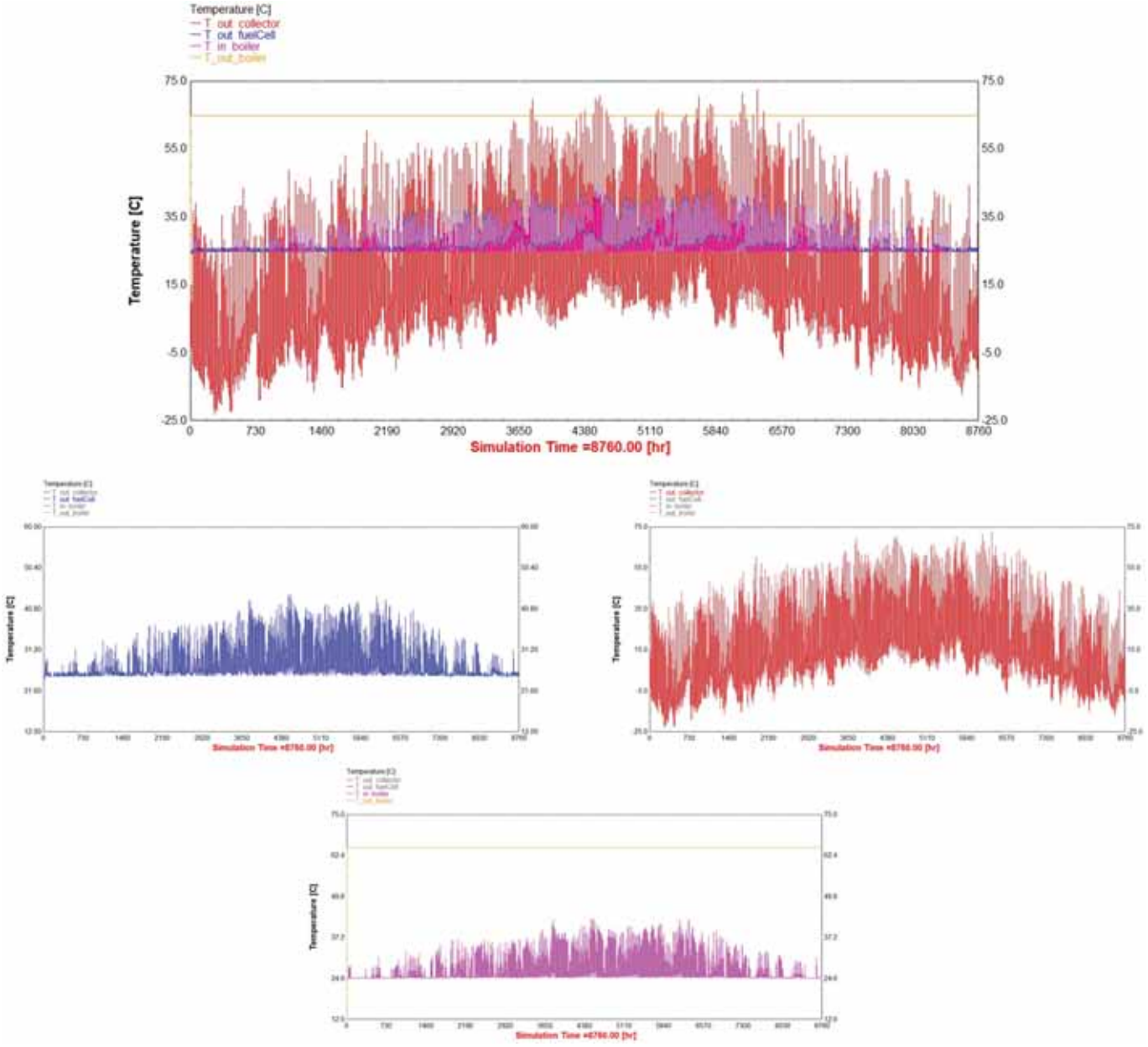

Fig. 23. Variation of the photovoltaic panel, fuel cell, and backup boiler temperature outlet during the year.

- To evaluate the effectiveness of the suggested approach, a complex of apartments with 12 and 13- floors buildings and four units per level was taken into consideration. There were 100 apartments in the building, each one a conventional living space of 196 square meters.
- The findings indicated that the system's performance may be improved by using two energy storage sources, such as a battery and a hydrogen tank, to accommodate the demands of residential structures.
- According to the results of the response surface method optimization, the annual cost of the system in comparison to the analysis was 674278.4 $, the annual comfort factor was 0.413%, the annual fuel consumption for the boiler was 41435.87595 m3/year, and the annual electricity consumption was −225694.7925 kW/h.
- The system's optimum panel count was 106, the ideal angle was 26°, the fuel cell power was 65.6 kW, the ideal number of wind turbines was 24, the heating capacity was 20.2 kW, and the cooling capacity was 48.7 kW, according to the optimization findings. The simultaneous, and variable decision-making increase in fuel cell power and Photovoltaic/thermal panel angle significantly increased overall electricity consumption.
- The increase in the number of wind turbines has increased the electricity consumption.
- Increase in Photovoltaic/thermal panel angle considerably decreased boiler fuel consumption.
- Increase in the power of the fuel cell significantly increased the fuel consumption of boiler.
- The findings revealed that the air temperature varies from 20 °C to 26 °C, demonstrating that the suggested system operates well all year round.

In conclusion, it should be noted that one method of storing energy created at one time and utilizing it at a later time using compressed air is via the use of batteries and hydrogen storage sources. It is possible to store energy generated during times of low demand to meet times of high need. When intermittent renewable energy sources like solar and geothermal energy are present, this technique has emerged as the most

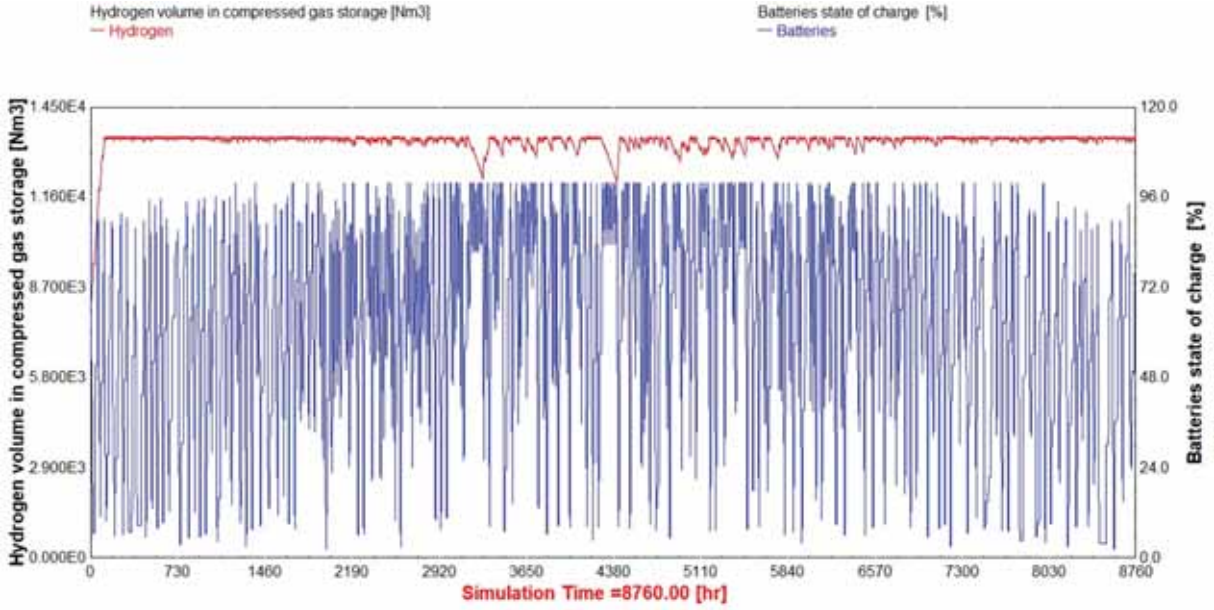

Fig. 24. Changes in the current of the hydrogen storage and the battery storage source.

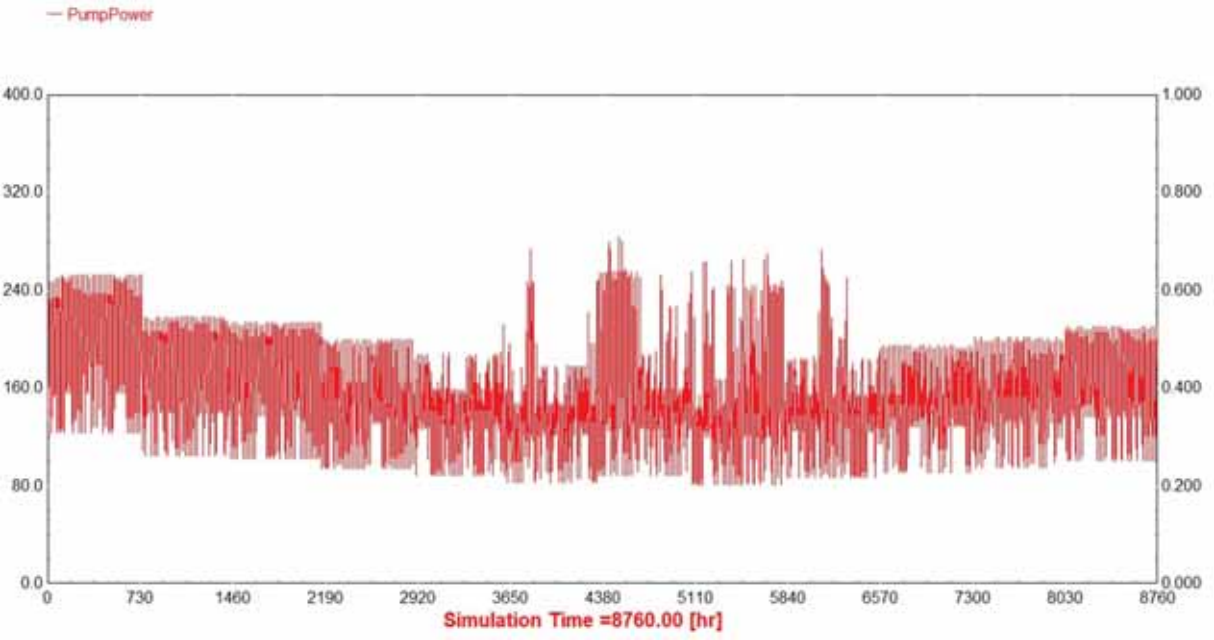

Fig. 25. Amount of fresh water produced during the year.

significant mode of energy storage. In order to ensure that power demands are supplied during peak hours, energy storage technologies may play a significant role.

5. Suggestions for future works

To enhance the scientific level of renewable energies as well as energy production systems and solve problems, suggestions were made to future researchers.

- The combination of organic Rankine cycles, Rankine steam and Brayton cycles to produce electrical energy and increase performance of the current proposed cycle.
- Possibility of launching the Current work system in multiple regions and continents of the world.
- Surveying the amount of exergy destruction of equipment and units of the proposed system and ways to minimize the amounts.
- Applying other cooling and heating production equipment like absorption chillers and comparing its results with the heat pump for cooling and heating products.
- The use of other renewable energies such as ocean thermal energy and the simultaneous examination of the use of several renewable energies.
- Use of new sources of energy reserves.
- Changing the type of solar receiver and checking the performance of the system with flat or parabolic plate collectors.

- Checking the performance of the system for supplying energy to buildings with a higher number of units.

CRediT authorship contribution statement

Ali Dezhdar: Conceptualization, Methodology, Software, Visualization, Investigation. **Ehsanolah Assareh:** Conceptualization, Methodology, Software, Visualization, Investigation, Supervision, Writing – review & editing, Data curation. **Neha Agarwal:** Writing – review & editing. **Ali bedakhanian:** Data curation. **Sajjad Keykhah:** Data curation. **Ghazaleh yeganeh fard:** Writing – review & editing. **Narjes zadsar:** Writing – review & editing. **Mona Aghajari:** Data curation, Software. **Moonyong Lee:** Supervision, Writing – review & editing.

Declaration of competing interest

The authors declare that they have no known competing financial interests or personal relationships that could have appeared to influence the work reported in this paper.

Data availability

Data will be made available on request.

Acknowledgement

This study was supported by the Priority Research Centers Program through the National Research Foundation of Korea (NRF) funded by the Ministry of Education (2014R1A6A1031189).

References

[1] P. Ahmadi, M.A. Rosen, I. Dincer, Multi-objective exergy-based optimization of a polygeneration energy system using an evolutionary algorithm, Energy 46 (2012) 21e31.
[2] H. Shakibi, et al., Exergoeconomic and optimization study of a solar and wind-driven plant employing machine learning approaches; a case study of Las Vegas city, J. Clean. Prod. 385 (2023), 135529.
[3] J.C. Lopez, A. Escobar, D.A. Cárdenas, Parabolic trough or linear fresnel solar collectors an exergy comparison of a solar-assisted sugarcane cogeneration power plant, Renew. Energy 165 (Part 1) (2021) 139–150. March 2021.
[4] A. Dezhdar, et al., A Transient Model for Clean Electricity Generation Using Solar Energy and Ocean Thermal Energy Conversion (OTEC) - Case Study: Karkheh Dam - Southwest Iran, Energy Nexus, 2023, 100176.
[5] E. Assareh, et al., Thermodynamic-economic optimization of a solar-powered combined energy system with desalination for electricity and freshwater production, Smart Energy. 5 (2022), 100062.
[6] S. Nikbakht Naserabad, et al., Thermal design and dynamic performance assessment of a hybrid energy system for an educational building, Energy Build. 278 (2023), 112513.
[7] F. Musharavati, et al., Multi-objective optimization of a biomass gasification to generate electricity and desalinated water using Grey Wolf Optimizer and artificial neural network, Chemosphere 287 (2022), 131980.
[8] O. Siddiqui, I. Dincer, Design and analysis of a novel solar-wind based integrated energy system utilizing ammonia for energy storage, Energy Convers. Manag. 195 (2019) 866–884.
[9] H. Gnaifaid, H. Ozcan, Multi-objective optimization of a concentrated solar energy driven trigeneration plant with thermal energy storage: a case study for Turkey, Case Stud. Therm. Eng. 20 (2020), 100642.
[10] M. Pinamonti, P. Baggio, Energy and economic optimization of solar-assisted heat pump systems with storage technologies for heating and cooling in residential buildings, Renew. Energy 15 (2020) 90–99.
[11] Y.E. Yüksel, Thermodynamic assessment of modified Organic Rankine Cycle integrated with parabolic trough collector for hydrogen production, Int. J. Hydrogen Energy 43 (11) (2018) 5832–5841.
[12] E. Assareh, et al., Techno-economic analysis of combined cooling, heating, and power (CCHP) system integrated with multiple renewable energy sources and energy storage units, Energy Build. (2022), 112618.
[13] E. Assareh, et al., An integrated system for producing electricity and fresh water from a new gas-fired power plant and a concentrated solar power plant – case study – (Australia, Spain, South Korea, Iran), Renewable Energy Focus. 44 (2023) 19–39.
[14] C. Chen, Q. Xia, S. Feng, Q. Liu, A novel solar hydrogen production system integrating high temperature electrolysis with ammonia based thermochemical energy storage, Energy Convers. Manag. 237 (2021), 114143.
[15] A.M. Behzadi, A. Habibollahzade, P. Ahmadi, E. Gholamian, E. Houshfar, Multi-objective design optimization of a solar based system for electricity, cooling, and hydrogen production, Energy 169 (2019) 696–709.
[16] M. Ozturk, I. Dincer, System development and assessment for green hydrogen generation and blending with natural gas, Energy 261 (2022), 125233.
[17] A. Izadi, et al., Design, and optimization of COVID-19 hospital wards to produce Oxygen and electricity through solar PV panels with hydrogen storage systems by neural network-genetic algorithm, Energy 263 (2023), 125578.
[18] E. Assareh, et al., Transient thermodynamic modeling and economic assessment of cogeneration system based on compressed air energy storage and multi-effect desalination, J. Energy Storage 55 (2022), 105683.
[19] E. Assareh, M. Assareh, S.M. Alirahmi, S. Jalilinasrabady, A. Dejdar, M. Izadi, An extensive thermo-economic evaluation and optimization of an integrated system empowered by solar-wind-ocean thermal energy converter for electricity generation – case study: Bandar Abas, Iran, Therm. Sci. Eng. Prog. 25 (2021), 100965.
[20] G. A' lvarez, M. Chagolla, J. Xama' n, M. Jime' nez, S. Sua' rez, M. Heras, A TRNSYS simulation and experimental comparison of the thermal behavior of a building located in desert climate, Energy Sustain. (2010) 349–356.
[21] J.F. Kreider, F. Kreith, Solar Energy Handbook, 1981.
[22] W. Yaïci, E. Entchev, K. Lombardi, Experimental and Simulation Study on a Solar Domestic Hot Water System with Flat-Plate Collectors for the Canadian Climatic Conditions. Energy Sustainability, American Society of Mechanical Engineers, 2012, pp. 69–78.
[23] Y. Allard, M. Kummert, M. Bernier, A. Moreau, Intermodel comparison and experimental validation of electrical water heater models in TRNSYS, Proc. Build Simul. (2011) 688–695.
[24] D. Brough, J. Ramos, B. Delpech, H. Jouhara, Development and validation of a TRNSYS type to simulate heat pipe heat exchangers in transient applications of waste heat recovery, Int. J. Thermofluid. 9 (2021), 100056.
[25] M. Rezvanpour, D. Borooghani, F. Torabi, M. Pazoki, Using CaCl2· 6H2O as a phase change material for thermo-regulation and enhancing photovoltaic panels' conversion efficiency: experimental study and TRNSYS validation, Renew. Energy 146 (2020) 1907–1921.
[26] S.A. Kalogirou, R. Agathokleous, G. Barone, A. Buonomano, C. Forzano, A. Palombo, Development and validation of a new TRNSYS Type for thermosiphon flat-plate solar thermal collectors: energy and economic optimization for hot water production in different climates, Renew. Energy 136 (2019) 632–644.
[27] K. Fong, T.T. Chow, C.K. Lee, Z. Lin, L. Chan, Comparative study of different solar cooling systems for buildings in subtropical city, Sol. Energy 84 (2010) 227–244.
[28] R. Shrivastava, V. Kumar, S. Untawale, Modeling and simulation of solar water heater: a TRNSYS perspective, Renew. Sustain. Energy Rev. 67 (2017) 126–143.
[29] K. Fong, C. Lee, Solar desiccant cooling system for hot and humid region–A new perspective and investigation, Sol. Energy 195 (2020) 677–684.
[30] A. Sohani, H. Sayyaadi, Thermal comfort based resources consumption and economic analysis of a two-stage direct-indirect evaporative cooler with diverse water to electricity tariff conditions, Energy Convers. Manag. 172 (2018) 248–264.
[31] E. Saedpanah, H. Pasdarshahri, Performance assessment of hybrid desiccant air conditioning systems: a dynamic approach towards achieving optimum 3E solution across the lifespan, Energy 234 (2021), 121151.
[32] A. Heidari, R. Roshandel, V. Vakiloroaya, An innovative solar assisted desiccant-based evaporative cooling system for co-production of water and cooling in hot and humid climates, Energy Convers. Manag. 185 (2019) 396–409.
[33] S. Rayegan, S. Motaghian, G. Heidarinejad, H. Pasdarshahri, P. Ahmadi, M. A. Rosen, Dynamic simulation and multi-objective optimization of a solar-assisted desiccant cooling system integrated with ground source renewable energy, Appl. Therm. Eng. 173 (2020), 115210.
[34] S.-H. Park, Y.-S. Jang, E.-J. Kim, Multi-objective optimization for sizing multi-source renewable energy systems in the community center of a residential apartment complex, Energy Convers. Manag. 244 (2021), 114446.
[35] N. Sommerfeldt, P. Ollas, in: Reverse Engineering Prototype Solar PV/thermal Collector Properties from Empirical Data for Use in TRNSYS Type 560. ISES Solar World Congress and IEA Solar Heating and Cooling Conference 2017, UAE, Abu Dhabi, 2017, pp. 1121–1132. October 29-November 2, 2017.
[36] A. Buonomano, F. Calise, M.D. d'Accadia, M. Vicidomini, A hybrid renewable system based on wind and solar energy coupled with an electrical storage: dynamic simulation and economic assessment, Energy 155 (2018) 174–189.
[37] H. Kim, J. Baltazar, J. Haberl, Methodology for Calculating Cooling and Heating Energy-Input-Ratio (EIR) from the Rated Seasonal Performance Efficiency (SEER or HSPF), 2013.
[38] Tess, Component Libraries V. 17.01 for TRNSYS V17. 0 and the TRNSYS Simulation Studio, Parameter/Input/Output Reference Manual, Thermal Energy System Specialists, LLC, 2004.
[39] S. Klein, B. Newton, J. Thornton, D. Bradley, J. Mitchell, M. Kummert, TRNSYS Reference Manual: Mathematical Reference, 2006.
[40] F. Oueslati, Hybrid renewable system based on solar wind and fuel cell energies coupled with diesel engines for Tunisian climate: TRNSYS simulation and economic assessment, Int. J. Green Energy 18 (2021) 402–423.
[41] R.F. Asrami, A. Sohani, E. Saedpanah, H. Sayyaadi, Towards achieving the best solution to utilize photovoltaic solar panels for residential buildings in urban areas, Sustain. Cities Soc. 71 (2021), 102968.
[42] E. Saedpanah, R.F. Asrami, A. Sohani, H. Sayyaadi, Life cycle comparison of potential scenarios to achieve the foremost performance for an off-grid photovoltaic electrification system, J. Clean. Prod. 242 (2020), 118440.

[43] H. ashidi, J. Khorshidi, Exergoeconomic analysis and optimization of a solar based hybrid system using multiobjective differential evolution algorithm, J. Clean. Prod. 170 (2018) 978–990.
[44] A. Nemati, M. Sadeghi, M. Yari, Exergoeconomic analysis and multi-objective optimization of a marine engine waste heat driven RO desalination system integrated with an organic Rankine cycle using zeotropic working fluid, Desalination 422 (2017) 113–123, 2017.
[45] A. Naseri, M. Bidi, M.H. Ahmadi, R. Saidur, Exergy analysis of a hydrogen and water production process by a solar-driven transcritical CO2 power cycle with Stirling engine, J. Clean. Prod. 158 (2017) 165–181.
[46] M. Dongellini, G.L. Morini, On-off cycling losses of reversible air-to-water heat pump systems as a function of the unit power modulation capacity, Energy Convers. Manag. 196 (2019) 966–978.
[47] T. Stehly, P. Beiter, P. Duffy, Cost of Wind Energy Review, National Renewable Energy Lab.(NREL), Golden, CO (United States), 2019, 2020.
[48] N. Sommerfeldt, H. Madani, In-depth techno-economic analysis of PV/Thermal plus ground source heat pump systems for multi-family houses in a heating dominated climate, Sol. Energy 190 (2019) 44–62.
[49] M.S. Saleem, N. Abas, A.R. Kalair, S. Rauf, A. Haider, M.S. Tahir, et al., Design and optimization of hybrid solar-hydrogen generation system using TRNSYS, Int. J. Hydrogen Energy 45 (2020) 15814–15830.
[50] A. Sohani, H. Sayyaadi, M. Azimi, Employing static and dynamic optimization approaches on a desiccant-enhanced indirect evaporative cooling system, Energy Convers. Manag. 199 (2019), 112017.
[51] R. Ghelich, M.R. Jahannama, H. Abdizadeh, F.S. Torknik, M.R. Vaezi, Central composite design (CCD)-Response surface methodology (RSM) of effective electrospinning parameters on PVP-B-Hf hybrid nanofibrous composites for synthesis of HfB2-based composite nanofibers, Compos. B Eng. 166 (2019) 527–541.
[52] Design Expert Software, V 13.0.5, Stat-Ease Inc, Minneapolis (USA), 2021.
[53] P.O. Fanger, Thermal Comfort. Analysis and Applications in Environmental Engineering. Thermal Comfort Analysis and Applications in Environmental Engineering, 1970.
[54] ASHRAE, Thermal Environmental Conditions for Human Occupancy, American Society of Heating, Refrigerating and Air-Conditioning Engineers, 2004.
[55] A.S. Nafey, M.A. Sharaf, Combined solar organic Rankine cycle with reverse osmosis desalination process: energy, exergy, and cost evaluations, Renew. Energy 35 (2010) 2571–2580.